# Magnetic fields in close white dwarf binaries

Erick C. Pastén

Instituto de Física y Astronomía
Facultad de Ciencias

Universidad de Valparaíso
Master en Astrofísica

September 2020
Valparaíso, Chile.

This thesis is solely my own composition,
except where specifically indicated in the text.



Erick C. Pastén
September 2020
Valparaíso, Chile.

# Acknowledgements

Thanks to my professors Matthias, Amelia and Monica who supported me strong on this travel.

To my family, specially my two most important women: mi mother and grandmother.

To my mates Catalina, Daniela, Ramses, Greko, Santiago y Martin for the laughs and the fights against the system; and my roommate Clara for putting on with me.

And my boyfriend Claudio, who is the most beautiful person i have ever met ...

# Abstract

White dwarfs are the degenerate remnants of stars that are born with initial masses $\lesssim 8-10\,M_{\odot}$ (e.g., Smartt et al. 2009 [63], Cummings et al.2019 [16]). Whereas the possibility that some of these stellar remnants possess strong magnetic fields was explored already in 1947 (Blackett et al. 1947 [9]), the observational confirmation occurred much later but still already 50 years ago (Kemp et al. 1970 [34]). It is now firmly established that a small fraction ($2-10$ per cent) of single white dwarfs exhibit magnetic fields of $B \gtrsim 1\,\mathrm{MG}$ (Hollands et al. 2015, Ferrario et al. 2015 [18], Kawka et al. 2010 [65]), and there is evidence that weaker fields are equally or possibly even more common (Landstreet & Bagnulo 2019 [39]). Interestingly, the fraction of magnetic white dwarfs is different for white dwarfs in binary stars and seems to depends on the binary configuration. A relatively large fraction ($\sim 30$ per cent) of cataclysmic variables, i.e. mass transferring systems, contains a strongly magnetic white dwarf, while they are nearly absent (less than one per cent) among detached white dwarf plus M dwarf binaries.

The origin of magnetic fields in white dwarfs is still debated, with current hypotheses including fossil fields (Angel et al. 1981 [4], Braithwaite & Spruit 2004 [10]), binary interactions either during a common envelope phase (Tout et al. 2008 [66]) or mergers (García-Berro et al. 2012 [24]), and processes internal to the white dwarf (Isern et al. 2017 [29]).

In this thesis I investigate magnetic white dwarfs in binaries observationally as well as theoretically. Weakly magnetic white dwarfs in close binaries may produce synchrotron emission which should be detectable with ALMA. I analysed ALMA observations of two close white dwarf binary stars finding evidence for synchrotron emission in one of them, while the interpretation of the observations of the other object remains unclear.

I combine my observational results with observations from the literature and theoretically investigate whether a crystallisation and rotation driven dynamo could be responsible for at least some of the detected magnetic fields in close binaries. I found

that indeed crystallisation might be important for understanding magnetic fields in close white dwarf binary stars and can most likely produce stronger fields than was previously thought. However, the rotation and crystallisation driven dynamo cannot explain the entire observed population of magnetic white dwarfs. For single white dwarfs, the merger scenario is most likely much more important.

# Contents

# CHAPTER 1

# Introduction

Close compact binary stars are among the most interesting objects in our Galaxy. In cataclysmic variables (CVs) a white dwarf (WD) accretes gas typically from a main sequence star companion. Depending on the magnetic field of the WD, either an accretion disk forms around the accreting WD or the overflowing material follows the magnetic fields lines and falls onto the poles of the WD. These objects are therefore prime object to study the physics of accretion disks and magnetic fields under extreme conditions. Other close compact binaries in which magnetic fields play a major role are Neutron star binaries. The spin down rates of pulsating Neutron stars in close binaries have been used to confirm angular momentum loss trough gravitational wave emission already in the last century (e.g Taylor et al. 1979 [23]) which has been awarded with the Nobel prize in 1992.

Close binaries with one compact object are also responsible for some of the most fascinating events in the Universe. They are the progenitor systems of Supernovae Ia (SN Ia) explosions and short gamma-ray bursts. The unique potential of SN Ia as distance indicators, sufficiently bright to serve as yardsticks on cosmological distance scales (e.g. Branch & Tammann, 1992 [76]), has made them some of the most important objects in the Universe and has led to the discovery of its accelerating expansion (Riess et al. 1998 [21]; Perlmutter et al. 1999 [55]), and eventually to the award of the 2011 Nobel Prize in physics. The detection of gravitational waves produced by two merging Neutron stars relates close compact binary stars also to another Nobel price

that has been given to astronomical research (Abbot et al. 2017 [2]).

This thesis is dedicated to study magnetic fields in close binary stars consisting of a WD and low-mass main sequence companion star. As most close compact binary stars, these WD binaries are formed through common envelope evolution.

## 1.1 The formation of close WD binary stars

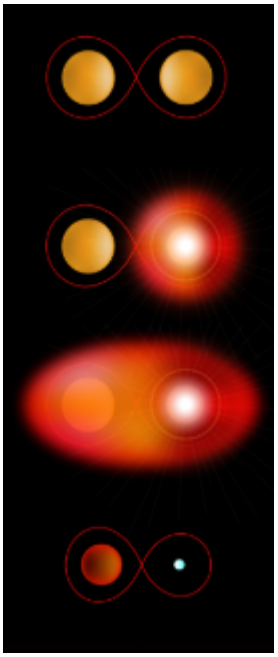

**Figure 1.1:** Evolution of a binary system into a PCEB. The stars go through a common envelope phase due to the great instability in the matter transference. The star reduces its distance dramatically as spiral-in process take place, as one of the components remain as a compact object, tipically a white dwarf.

Roughly half of all stars are born in binary stars and a significant fraction of these binaries interact through mass exchange at different times during their stellar evolution. The most important process for the formation of close binary stars is common envelope evolution (e.g. Paczynski et al. 1976 [50]). When the more massive star of a main sequence binary system evolves into a giant star it may fill its Roche-lobe which then leads to Roche-lobe overflow. This mass transfer is dynamically unstable, i.e. mass transfer rate generates more mass transfer on the dynamical time scale. The resulting runaway process leads to mass transfer time scales much shorter than the thermal time scale of the accreting star. This implies that the overflowing mate-

rial cannot be incorporated and instead a common envelope forms around the core of the giant star (the future WD) and the main sequence star. Drag forces between the stars and the material produce a transfer of energy to the envelope, leading through a *spiral-in* process. The envelope begins to expand due to the energy input and is finally ejected into space. The outcome of this common envelope evolution is a post common envelope binary (PCEB): a very close binary system composed of at least one compact object (in most cases a WD) and a companion star. Figure 1.1 illustrates the formation of PCEBs containing one WD. Some binaries that form through common envelope evolution contain strongly magnetic WDs (MWDs) with field strengths of up to several hundred MG. In this thesis I investigate the possible origin of these magnetic fields and their detectability with ALMA. In the following sections I describe the state of the art of MWDs research.

## 1.2 Single MWDs

The first MWD was the detected exactly 50 years ago through circular polarized light emitted by GRW +70 8247 (Kemp et. al 1970 [34]). Today we know that a relatively large fraction of WDs are strongly magnetic. Most MWDs are hydrogen-rich (DA). They are classified as DAp or DAH, indicating the method used for the discovery of their magnetic nature (polarization or Zeeman splitting). The rapid increase in MWD discoveries came through surveys such as the Hamburg/ESO Quasar Survey (HQS, Wisotzki et al. 1991 [73]), the Edinburgh-Cape survey (Kilkenny et al. 1991 [37]), and the Sloan Digital Sky Survey (SDSS, e.g., York et al. 2000 [74]). Today we know around 600 isolated MWDs with magnetic fields in a range of $10^3 - 10^9 G$ (Kawka, et. al 2020 [20]). The current knowledge of single MWDs can be summarized as follows:

1. 10–20% of WDs are magnetic according to volume-limited samples (Kawka et al. 2007 [33]; Giammichele et al. 2012 [25]; Sion et al. 2014 [62]), but only 2–5% in magnitude-limited samples (Liebert et al. 2003a [41]; Kepler et al. 2013, 2015 [35]). This discrepancy may be understood because on average MWDs are more massive an colder that the non-magnetic ones, i.e they have lower luminosities.

2. Although the reason is not clear, there is a paucity of MWDs (see Fig. 1.2) in the intermediate field range (0.1–1 MG, see Kawka and Vennes 2012 [70]). The magnetic field distribution could be bi-modal exhibiting a high field (1–1000 MG) population and a low field ($< 0.1$ MG) one (Ferrario et al. 2015 [18]).

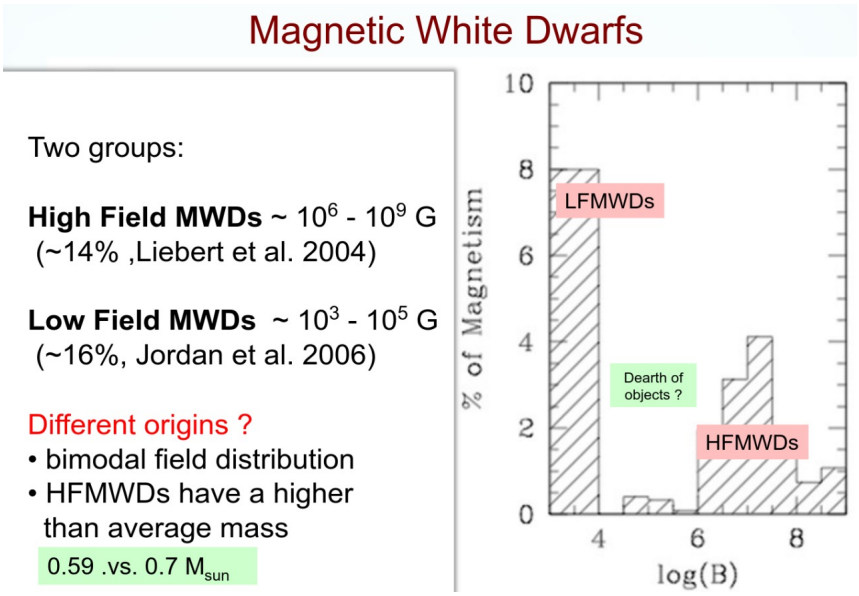


**Figure 1.2:** Bi-modal distribution of field strength in MWDs

3. Strongly MWDs are, on average, more massive and older/colder than non-magnetic WDs (e.g. Kepler et al. 2013 [35]; Kawka 2020[20]; Kilic et al. 2020 [36]; McCleery et al. 2020 [45]).

4. McCleery et al. (2020) [45] analysed the population of WDs within 40 pc and, in addition to finding a higher average mass for magnetic DA WDs, they also found an increase in the incidence of magnetism among WDs with decreasing effective temperature and increasing log(g) (i.e. increasing mass). However, the authors also mentioned that the latter should be taken with caution given the poor number statistics (only 24 magnetic DA WDs in their sample).

5. Kepler et al. (2013) [35] studied the incidence of magnetism in hydrogen-rich (DA) WDs within the SDSS and found an increase in apparent WD masses for increasing magnetic field (their Figure 14) and also an increase in the field strength for the coldest WDs ($T_{\rm eff} \leq 13\,000$ K, in their Fig. 11).

## 1.3 MWDs in binary stars

Interestingly, the fraction of MWDs is very different for single WDs and those that are part of a binary system. In addition, it even seems that the fraction of MWDs depends on the type of binaries. The High-field magnetic WDs (HFMWDs) detected are com-

monly found in interacting binaries, in which the degenerate star accretes mass from a non-degenerate companion (magnetic CVs). In contrast, very few of the detached progenitors of this kind of stars seem to contain a strongly MWD.

Among the interacting MWD binaries, there are polars and intermediate polars (IPs). In IPs the magnetic field is not strong enough to dominate the accretion at all scales and an accretion disk forms. This accretion disk is then disrupted at smaller radii by the magnetic field. In polars, the overflowing matter is channelled onto the MWD surface by magnetic streams (e.g., Ferrario and Wehrse, 1999 [19]). The evolution of magnetic and non-magnetic CVs is expected to be similar, but according to Li et al. (1994) [40], and Belloni et al. 2020 [7] magnetic braking is not as effective in strongly magnetic CVs because the magnetosphere of the MWD traps the companion star's wind. This hampers the angular momentum loss, thus reduces the mass transfer rate and leads to longer evolutionary timescales.

The only detached close WD binaries containing a MWD are the so-called *low accretion rate polars* (LARPs) (e.g. Schwope et al. 2009 [46]). In these systems accretion occurs from the wind of the companion star, which is close to fill its Roche lobe. In the majority of them, the spin of the MWD is synchronized with the orbital period( Webbink Wickramasinghe 2005 [71]). These systems are sometimes also referred as *pre-polars*, i.e. assumed to be progenitors of polars. However, one of the biggest mysteries in the field of MWDs is that all these LARPs (or pre-polars) contain very cold (and therefore old) WDs. Among the young (containing hot WDs) detached close WD binaries not a single strongly MWD has been found despite the fact that several hundreds of these objects are known.

## 1.4 Theories for magnetic field generation in WDs

Currently there are four possible scenarios that try to explain the origin of HFMWDs:

1. Fossil Field hypothesis (e.g. Angel et al. 1981 [4]; Wickramasinghe & Ferrario 2005 [17]): According to this scenario, HFMWDs would descend from Ap and Bp main-sequence stars with initial masses in the range $\sim 1.5 - 8.0\, M_{\odot}$ (e.g., Angel et al. 1981 [4]). These stars are known to have magnetic fields between $10^3$ and $10^5$ G on the main sequence, which can be translated into fields in excess of 10 MG when the star becomes a WD, assuming magnetic flux conservation. However, Kawka & Vennes (2004) [32] questioned the validity of this assumptions

based on updated observational constraints. Aurière et al. (2007) [5] performed spectropolarimetric surveys revealing in turn that this scenario cannot explain the birth rates of HFMWDs. A physical difficulty this scenario faces is related to the magnetic flux conservation. It is not clear under which conditions the fossil magnetic flux could be fully preserved till the WD formation. For instance, a large fraction of the flux could be carried away by the envelope. Additionally, several very complicated processes operating in a star, e.g. rotation, convection and field topology, as well as the presence of a companion star, might strongly affect the flux conservation or how the field attenuated in the envelope arises to the core. The fossil field scenario might provide magnetic fields for some WDs, but should lead to negligible fields (below 1 kG) for the overwhelming majority of them.

2. Dynamo generated during common-envelope evolution in close binaries (e.g. Regős-Tout 1995 [57]; Nordhaus et al. 2011 [47]; Wickramasinghe et al. 2014 [72]): According to this scenario the magnetic fields of WDs in close binaries are generated during the common envelope phase. The possible amplification of the field in this scenario is based on the transfer of orbital energy and angular momentum during spiral-in. Coupled with convection, this leads to large-scale magnetic field amplification via dynamo; The dynamo converts free energy in differential rotation into magnetic energy. The multiples models consider the differential rotation generated in different places of the star (in the common envelope itself, an accretion disk, or in the outer layers of the degenerated core). However, this scenario is not free of problems (see Briggs et al. 2018a [11], Temmink et al. 2020 [65], Belloni et al. 2020 [7])

3. Coalescing double degenerated cores (e.g. García-Berro et al. 2012 [24]): The field generation could occur when two degenerate cores coalesce, which might happen for interacting binaries such as double WDs, WD+red giants and double red giant binaries. These authors showed that a hot, convective and differentially rotating corona, present in the outer layers of the object formed due to merger, last long enough to produce magnetic fields consistent with observations of single HFMWDs, providing WD masses consistent with observations. However, the fraction of HFMWDs originated through such a channel is expected to be very small, and this scenario only works for single WDs and cannot account for the high frequency of MWDs among CVs. García-Berro et al. (2012)

[24] and Temmink et al. (2020) [65] carried out single/binary population models and found in both cases that the fraction of merged double degenerate cores and double WDs in the solar neighborhood is only $\sim$ 3 per cent. Considering this, coalescing of double degenerate cores seems to be the less important channel towards MWDs. However, it could be much more important among the most massive WDs.

4. WDs core crystallization with age (e.g., Isern et al. 2017 [29]): During the cooling process that follows the WD formation, the ions in the core of the WD begin to freeze in a lattice structure (van Horn 1968 [69]). A typical WD is composed mainly of Carbon and Oxygen. Oxygen crystallizes at a higher temperature than Carbon, creating an Oxygen-rich solid core surrounded by a convective liquid mantle, mostly composed by Carbon. This mantle produces a dynamo that allows the creation of a magnetic field in case the WD is rotating relatively fast. Direct observational evidence of crystallization at the core of WDs was recently observed by Tremblay et al. (2019) [67] as a delay in the cooling sequence of WDs due to the releases of latent heat as the cores of the WDs crystallize. This process is initiated much faster for the more massive WDs, an is therefore a promising scenario to explain why MWDs are, on average, more massive and cooler.

## 1.5 Aim of this thesis

In this work, I will focus mainly on two topics related to MWDs that can provide new constraints on the origin of WD magnetic fields:

1. External radio-mm emission in some PCEBS and its explanation: Radio and mm emission have been detected in multiple PCEBs. Although there is no big evidence of high magnetic fields in this stars, this new emissions could be indirect evidence of magnetic activity and can provide us important information about the evolutionary path of magnetic interacting binary stars. I will present new ALMA data of PCEBs and discuss the implications for magnetic fields of WDs in PCEBs.

2. New calculations and assumptions in crystallization theory: Developing and investigating the new theory of core WD crystallization and its observational evidence, it is possible to find new theoretical assumptions about the physical

parameters related to this process. It seems that the field strengths predicted by this model could increase with the new assumptions.

# CHAPTER 2

# Observations

## 2.1 ALMA observations

The *Atacama Large Millimeter Array* (ALMA) is a group of multiple antennas placed on *Chajnator*, a plane localized in the North of Chile. ALMA allows to perform interferometric observations at mm wavelengths. The spatial resolution and the sensitivity of ALMA are unparalleled in this wavelength range. In this thesis I will discuss ALMA observations of two PCEBs: NN Ser and V471 Tau. Observations of the also intriguing PCEB named QS Vir have been performed but will be analysed separately and its results will be given in future works.

### 2.1.1 NN Ser

NN Ser is a relatively young PCEB with a cooling age of the WD corresponding to only $\sim$ 1.3 *Myrs* (Schreiber & Gänsicke 2003 [60]). The companion to the WD is an M-dwarf of spectral type M4. Both stars orbit their common centre of mass within 0.13 days (Brinkworth et al. 2006 [12];Parsons et al. 2010a [53]). The system displays eclipse timing variations (ETVs) that are well fitted by two planetary mass bodies (Beuermann et al. 2010 [8]). The fact that the existence of two circumbinary planets very well fits the eclipse timing variations, led to speculations whether these planets might have survived common envelope evolution or if they perhaps formed from

the leftovers of the common envelope. The latter scenario motivated the first ALMA observations of NN Ser with the idea that a second generation proto-planetary disc composed of cold dust surrounding the binary star could still be detectable.

### First observations with ALMA

The ALMA observations were conducted on 2014-04-30 and repeated on the 2015-01-22, as the rms sensitivity of the data did not reach the requested value of 25 µJ in the first instance. No flux was detected in the first observation but the second data set showed a significant detection. In the latter, the single continuum mode in Band 6 was used, implying a total bandwidth of 7.5 GHz with individual channel widths of 15.625 MHz. 39 antennas were used, with minimum and maximum baselines of 15.1 m and 348.5 m respectively. The calibration sources associated with these observations were J1337-1257 for band-pass calibration, and J1550+0527 for phase calibrations. The observations consisted of 5 scans of 6.87 min each, translating to a total time on the science target of 34.35 min. Standard calibration steps were applied to the data, and the resulting visibilities were deconvolved using the CLEAN algorithm with natural weighting to create the final image. The observations led to a detection with a flux value of $0.11 \pm 0.03$ mJy at 1 300 µm (see Fig. 2.1 taken from Hardy et al. 2016 [27]).

While this result supported the original hypothesis of second generation dust in a circumbinary disk, these observations alone were not sufficient to draw final conclusions about the nature of the detection because two interpretations remained possible. A detection at mm wavelengths could be explained via magnetic emissions (like gyrosynchotron) or thermal emission of dust from the circumbinary disk.

### Second observations with ALMA

The second observations were taken on 2016-12-29 at band 4 and 2017-03-27 at band 7. The most important specification of the reduction process are:

1. **Band 4:** Removed antenna DA55 from one of the observations as state in README.txt file. Imaging processed over aggregated bandwidth ($7.5GHz$) of spw 17, 19, 21 and 23. $7.4\frac{\mu Jy}{beam}$ of Rms reached.

2. **Band 7:** No manual flags performed. 0.033 mJy/beam of rms reached at the of 7.5 GHz.

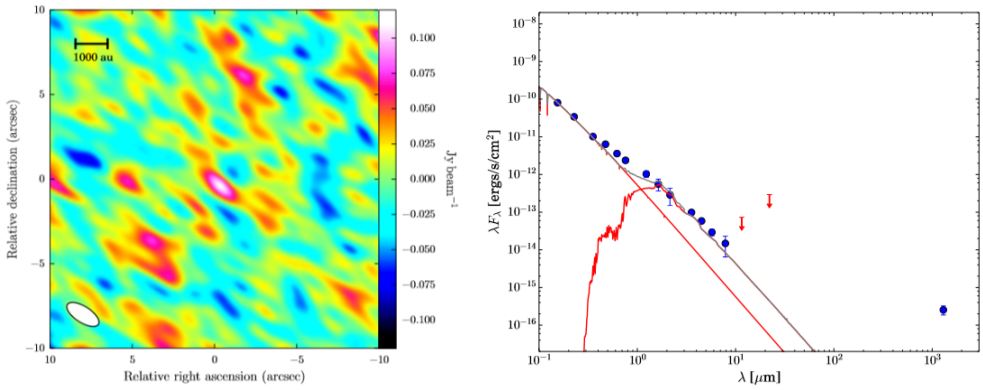


**Figure 2.1:** *Left*: First detection on band 6 of NN Ser. *Right*: Spectral energy distributional of NN Ser at the end of the WD eclipse. The red lines denote fluxes from a model 60 000 K WD and M4 main-sequence star, with the grey lines as their sum. The blue points are the data, and the red arrows are upper limits from WISE. There is a marginal excess above the stellar photosphere in the range 0.47-0.75 µm, but this may be the result of heating of the main-sequence star by the WD. An excess at 1 300 µm is clearly detected however.

Imaging procedures were performed using the **mfs** mode with the latest version of CASA available and standard calibrations.

In both bands, no flux was detected at the position of the target, related with the respective rms of each detection (Fig. 2.2).

### 2.1.2 The case of V471 Tau

V471 Tau is a compact binary star composed by a WD and a K-star. The orbital period is around 12h and they are separated by an approximate distance of 1 solar radius. V471 Tau represents one of the most studied compact binary stars, being a point of support for the study of the evolution of binary stars in general. However, it still shows many mysteries for researchers. In 1996, monitoring was performed throughout two complete orbital periods with VLA in 4 frequency bands (J. Lim, 1996 [42]). The data showed an eclipsing emission at these frequencies drawing strong attention. Explanations based on synchrotron radiation occurring between both stars were proposed. However, over the years, this phenomenon has not been fully explored but it may offer the potential to better understand magnetic field dynamics in these binary stars. Here I present ALMA observations of this target which allow to further test the hypothesis of synchrotron emission being responsible for the Radio detection.

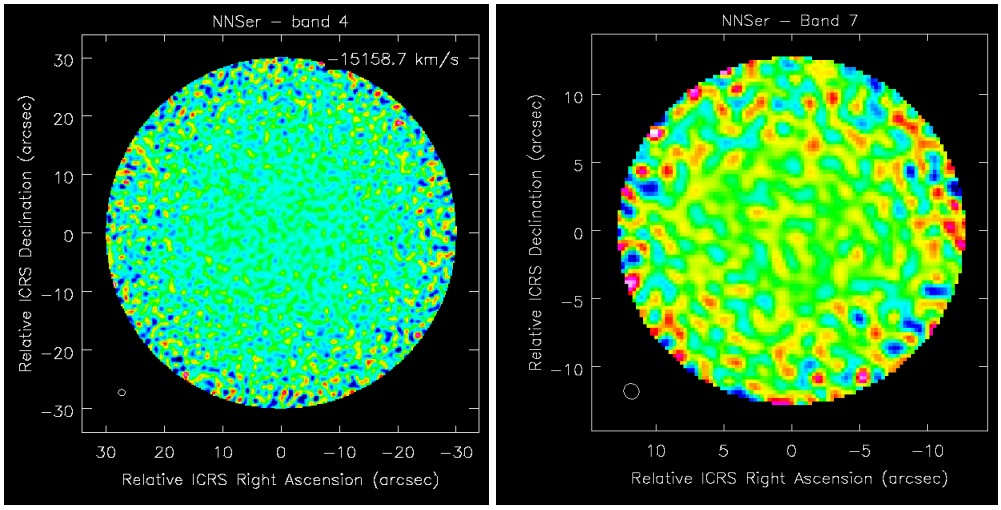


**Figure 2.2:** Non-detection in band 4 and 7 on NN Ser

2 observations of V471 Tau with ALMA in band 6 were performed at 2016 (2.3). I downloaded the data from the ALMA Archive Query page. Measurements were made in 2 sections of 1 hour each on different days. The *scriptforPI* file was made for version 4.7.0 of CASA, so it was necessary to download this version. Due to the large size of the data, the procedure was carried out in the KOSMOS cluster at the Universidad de Valparaíso.

Data is reduced using scriptforPI file with CASA 4.7.0. No errors or warnings occurred during the process. The reduction returns a single file which contains both observations.

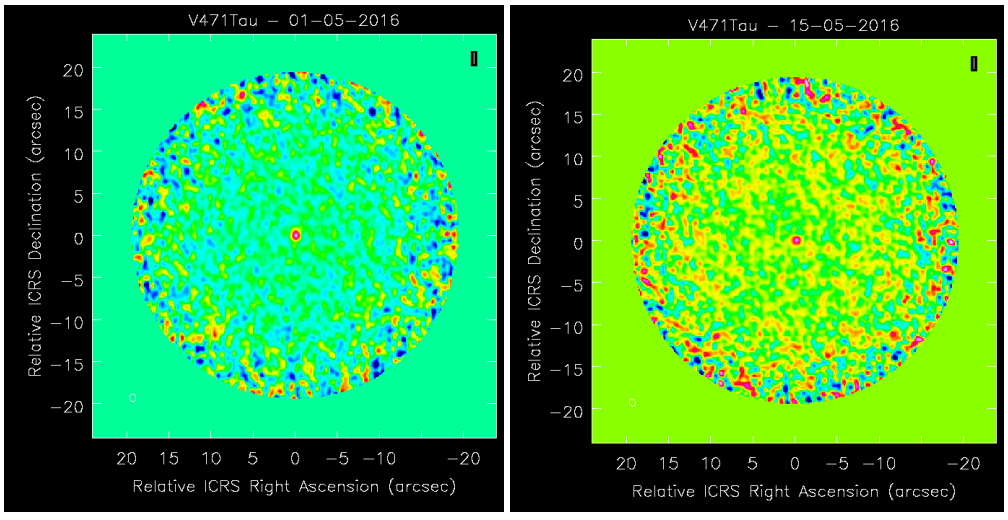


**Figure 2.3:** The two detections on V471Tau in band 6

### Continuous, spectrum and temporal evolution detection

Imaging procedures are performed with the **mfs** mode with the latest version of CASA available. There are 3 different procedures: a total collapse mode for all the observation, during all the time and all the frequencies of the band; collapses through spectral windows that allow studying the shape of the emission spectrum; and collapses by time intervals that will permit to measure variability of the emission, verifying the consistency with the phases of the eclipse according to the ephemeris measured at optical wavelength. A total collapse is also performed in cube mode to verify or rule out the presence of emission lines, finally showing the absence of those. The parameters for general collapse are detailed below.

### Observation 1

The task was performed using the star V471Tau. The imsize used is 360, along with a cell size of 0.14 arcsec. Detection gives a value of $2.04 \pm 0.096$ mJy of integrated flux.

### Observation 2

An imsize of 432 and a cell size of 0.11 arcsec were used. The detection yields a value of $1.75 \pm 0.13$ mJy. For the comparison between the data divided by spectral band and time, the *tclean* task is performed with 500 iterations. Then, an *imsmooth* is performed between the images with the lowest resolution in order to balance the shape of the SB, improving the reliability of the results.

### Spectral windows collapse

Spectral window collapses were made for both observations. The data has four spectral windows, the last one containing the largest channels. The data are presented in Table 2.1 and the corresponding plots in Fig. 2.4.

| Flux OBS1 [mJy] | Error [mJy] | Flux OBS2 [mJy] | Error [mJy] |
|---|---|---|---|
| 1.98 | 4 | 2.09 | 0.27 |
| 2 | 10 | 1.87 | 0.26 |
| 2.3 | 3 | 2.04 | 0.27 |
| 1.94 | 0.25 | 1.3 | 0.23 |

**Table 2.1:** Data obtained from spectral division.

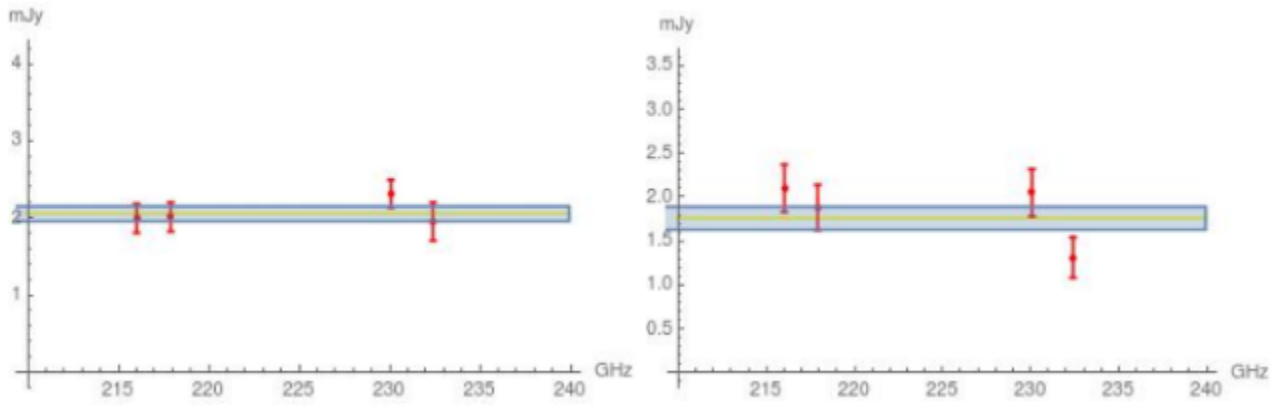


**Figure 2.4:** The frequency of the detected flux for both observations. The yellow line represents the value detected in the total collapse with its respective error shown by the shaded region.

### Time-lapse collapse:

For both observations, collapses are made at time intervals of approximately 1 min. The data has five integrations for each observation with different Field IDs, taking advantage of this fact for the process. The data are presented in Table 2.2 and Fig. 2.5.

| Flux OBS1 [mJy] | Error [mJy] | Flux OBS2 [mJy] | Error [mJy] |
|---|---|---|---|
| 2.37 | 0.24 | 2.03 | 0.29 |
| 2.73 | 0.21 | 1.57 | 0.24 |
| 1.38 | 0.19 | 1.97 | 0.35 |
| 2.32 | 0.21 | 1.82 | 0.28 |
| 1.65 | 0.2 | 1.73 | 0.29 |

**Table 2.2:** Data obtained from temporal split

The observations leave enough questions to answer:

1. The total integrated emission is stronger in one observation than in the other. If we calculate the phases of the eclipse where the observations were made with the ephemeris function of V471Tau, we can see that it is in agreement with what was seen in 1996 with VLA (Fig 2.3).

2. The emission is slightly stronger at millimeter wavelengths than in the radio wavelengths range. Following previous investigations with VLA at 2, 3.6 and 6

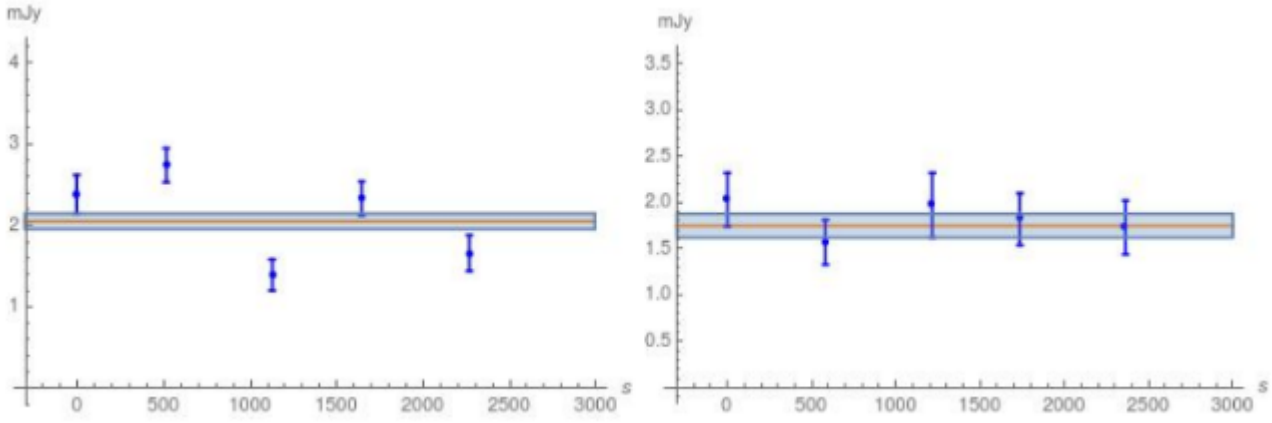


**Figure 2.5:** Detected flux as a function of time for both observations. The time in which the first integration was made is taken as 0. The orange line represents the value detected in the total collapse with its respective error shown by the shaded region.

cm, a value of between 1 and 1.2 mJy can be estimated for the strongest eclipse window.

3. The 1996 spectral index was estimated as flat ($\alpha \sim 0$). Because the current emissions detected in the millimeter band are stronger, it is then possible that this spectral index is slightly positive.

4. The location of the critical frequency. This value would allow you to set dimensions such as the magnetic field and the electron density of plasma.

5. The study of the polarization of the emission is pending. The author is currently investigating how to extract parameters and polarization percentages to support the hypothesis of the magnetic character of the emission. However, we need to make another proposal to study this kind of features because the current data does not allow to perform this task.

# CHAPTER 3

# Radio emission and its magnetic origins in binary stars

In what follows I investigate whether the previously presented observational results support the idea that ALMA and Radio detections of PCEBs are strongly related to *magnetic proccesses*.

The origin of the radio emission in this kind of binary stars could be explained by different mechanism. As we will see, the thermal emission hypothesis can be excluded based on our observations. Then, the best explanation that remains are indeed non-thermal emission due to magnetic processes.

## 3.1 The NN Ser case

The first ALMA band 6 detection of NN Ser was atributted to thermal emission of cold dust (Hardy et al. 2016 [27]), possibly originating from a second generation debris disc that formed from the remaining of common envelope material.

Due to the posterior non-detections at band 4 and 7 analized in this work, we need to discard the cold dust hypothesis. This is because the cold dust can not disappear on time scales as short as two years. In addition, the more recent band 4 and band 7 observations were more sensitive than the initial band 6 observations. The only

remaining possibilities to explain the observations are that we have observed a transit event or that the first detection represented a false positive.

### 3.1.1 Eclipsed synchrotron emission

Concerning the first, the possibility exists that the emission could be of a magnetic origin due to material moving through the magnetic fields in the middle of the stars. The non-detections could then represent eclipses of the emission region due to the secondary star. To test this last possibility, we performed a comparison between the phases of the eclipse based on the ephemeris of NN Ser [44]:

$$T = T_o + PE + \beta E^2, \tag{3.1}$$

$T_o = 52942,9338$ (MJD), $P = 0.13008014$ and $\beta = 10^{-12}$.

If this is the explanation, then the time of our detection should be placed around the non-eclipse phase; and the non-detection should correspond to eclipse phases. This could explain why we have detection and non-detection at different times. If we put those values in the ephemeris function, we can compare the eclipse times with the observing times. We present this in (Fig. 3.1).

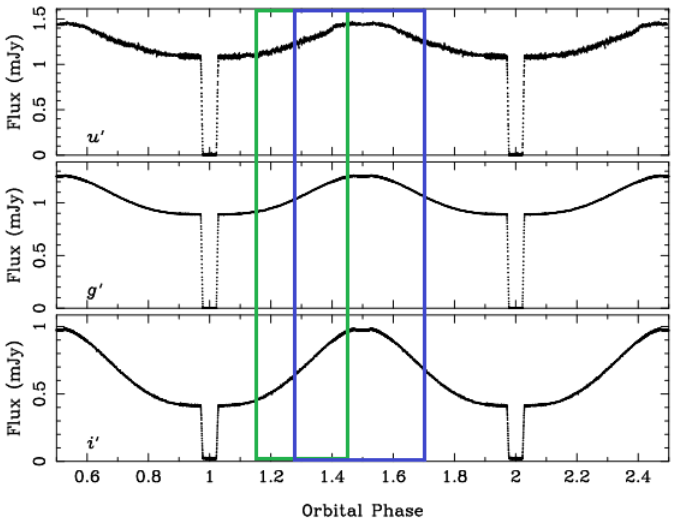


**Figure 3.1:** Detection of 1.3 mm (Green) and posterior non-detection (Blue) in NN Ser matched with eclipse phase. It does not seems to exist any relation between eclipse dynamics and the emissions.

As we can see, the detection and non-detection times do not fit with the corre-

sponding eclipse phases. We can therefore dismiss the gyrosynchotron emission in the middle of the stars as a cause of this behaviour. We have two more possible explanation for this.

### Millimeter flare

Another interesting transient phenomenon that potentially could provide a reasonable explanation for the observations in NN Ser is that it could be a millimeter flare. Proxima Centauri is the nearest star to our solar system and has been detected at 1.3 mm (MacGregor et al. 2017 [43]). Proxima Centauri is a M-type star that showed a peak in its emission of $100 \pm 4\ mJy$. Due to the duration of the emission, its spectral index and polarization, it has been concluded that the data is likely explained by a millimeter flare originating from the convective star.

As we do not have sufficient rms to split the emission in time units and no polarization information of our data in NN Ser, we can verify if this hypothesis is still useful based on the flux of emission. To do that, we need to notice that NN Ser is placed at $1670 \pm 141$ light yrs and Proxima is much closer (at $4.22 \pm 0.01$). So, if we consider that the physical origin of both emissions corresponds to the same mechanism (as we know that both stars are of the same M-type), then the emissions should be similar in flux. If we do a rough proportionality test using the inverse square law we can obtain the expected value of flare emission localized at the distance to NN Ser:

$$\frac{I_{Proxima} * R^2_{Proxima}}{R^2_{NN\ Ser}} = \frac{100 * 4.22^2}{1670^2} \sim 0.00064 mJy \tag{3.2}$$

Our detection in NN Ser was $\sim 0.11$ mJy, a value almost 180 times the expected by comparison. We conclude that a flare seems to be unlikely the mechanism behind the detection. However, we cannot completely rule out this scenario as factors as the magnetic activity of NN Ser could be increased (e.g., due to the fast rotation of the M dwarf), and therefore, increase the flux emission of the flare.

### False positive

As we can discard the cold dust scenario and the synchrotron scenario and as the megaflare hypothesis seems unlikely, we should consider a more technical explanation for the detection. The statistical confidence level of the detection in the band 6 was relatively low ($3.6\,\sigma$). Therefore, the possibility of a false positive detection in the observations is very small (aproximattely 0.0003% ) but it remains a possibility if we

are not able to derive another conclusion. We are currently re-reducing the first ALMA data using data reduction tools that were not available in 2016 to further investigate the possibility that the detection was perhaps a false positive or maybe even the result of sub-optimal data reduction techniques.

## 3.2 The V471 Tau case

V471 Tau is a member of Hyades cluster. The WD in V471 Tau has puzzled astronomers for decades. The fact that it is the hottest (and therefore youngest) and at the same time the most massive WD in the cluster indicates that its evolutionary path was most likely affected by mass transfer phases beyond common envelope evolution (Jensen et al. 1986 [31]).

The possibilities of interaction between the components in V471 Tau has been enhanced long time ago by the eclipsing radio emission detected by Lim et al. 1996 [42]. They presented strong evidence confirming the presence of eclipses in the centimeter (2, 3.6 and 6 cm) radio emission (VLA) of the eclipsing binary. This emission was in agreement with the optical eclipse, and showed 2 deeps and 2 peaks. The flux density outside the eclipse was $\sim 1\ mJy$, and shows little difference between the first and the second eclipse windows. The radio spectrum appears to be flat between 6 and 2 $cm$.

To verify if our data is in agreement with this kind of emission, we perform an analysis with the ephemeris function [48] to see if the emission are in the same phase that are the peaks in the 1996 detection.

The ephemeris function is:

$$T_o = HJD2440610,05693 + 0,52118373E \tag{3.3}$$

As we see in Fig. 3.2, our detections are in the same phase that are the peaks observed in the Lim et al. 1996 [42]. It seems plausible that both emissions have the same origin.

### 3.2.1 Geometry and physical scenario of the emission

The source of emission has been studied by Lim et al. 1996 [42]. Due to the eclipsing nature, they considered 2 possibilities:

1. The source is just above the K dwarf

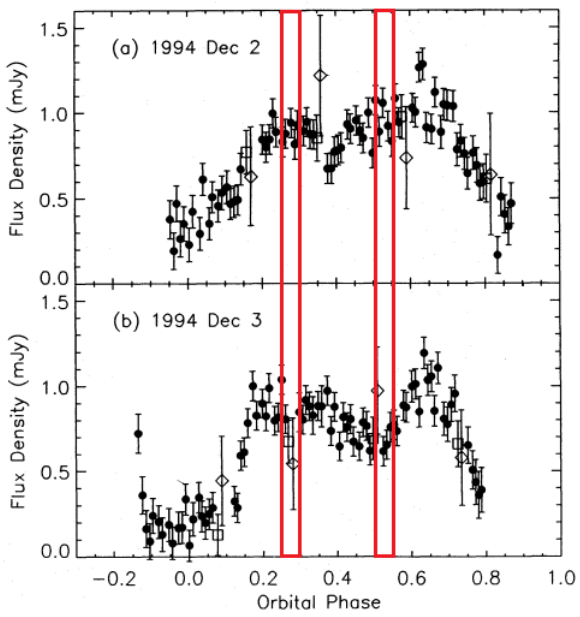


**Figure 3.2:** Eclipsing emission detected in V471 Tau at 1996. Red boxes represent the phases of the eclipse in which recent observations were made with ALMA. It can be seen that the time interval in which these emissions occur agrees with the previous ones, which correspond to the phases where the center of the two stars can be seen. It is also confirmed that one window of the eclipse has stronger emission than the other, in the same way that observation 1 is stronger than observation 2.

2. The source is in the place of WD

There are 3 main reasons to discard the second possibility:

1. The radio source must be significantly larger than the WD for the eclipse width to exceed $\Delta\phi = 0.066$ (the photospheric eclipse width of the eclipse). According to Lim (1996), the source has to be 4.5 times the radius of the WD. This size cannot reproduce the shape of the observed eclipse.

2. The X-ray emission detected (Jensen et al. 1986 [31]) in V471 Tau show narrow dips attributed to gas trapped at the Lagrangian points (L4 and L5 in 3.3), located at $\phi = 0.83$ and $\phi = 0.17$, which are approximately the orbital phases where the eclipse begins and ends. This gas only absorb partially the hypothetically WD radio-emission. However, the radio light curve does not return to its un-eclipsed level between these absorption events and the eclipse of the WD, meaning that the source has to be at least 1.9 $R_{\odot}$.

3. Rotational modulation in optical and X-ray light curves has been interpreted as coming from accretion of heavy elements through the magnetic poles of the WD. There is no detectable $\pi$ or $\sigma$ Zeeman sub-components in its Lyman $\alpha$ photospheric absorption line, which means that the field cannot exceed a few kilogauss. This implies that the field reaches a low value very close to the WD, meaning that beyond this point the radio emission becomes optically thin. This small shape is contrary to the large source required by the other points to explain the WD radio emission.

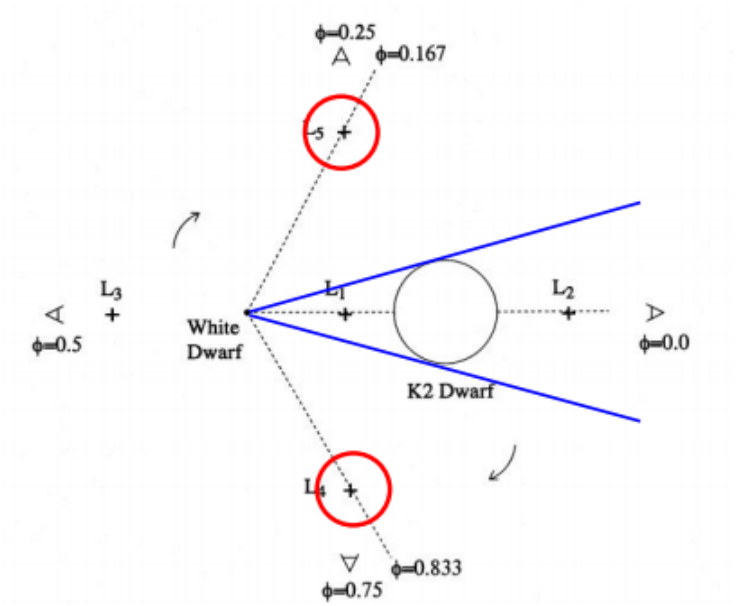


**Figure 3.3:** Main aspects at the supposition of being the WD emitting the radiation. In blue the angle of the full eclipse and in red the Lagrangian L4 and L5 points that absorbs X-ray emission in Jensen et al. 1986 [31]

Another interesting aspect that perhaps helps to understand the nature of the radio emission, is that we can discard the thermal origin of this emission; for a source of circular cross section, the depth of the eclipses implies an average brightness temperature of $T \geq 8.2 \times 10^9 K$. This temperature seems to be the upper limit expected for non-thermal gyrosynchrotron or synchrotron emission if the source is significantly smaller.

Two possible physical origins to this non-thermal emission have been proposed: enhanced solar-like activity in the K-dwarf corona or a direct association with the binary nature of V471 Tau.

1. **Active solar-like K-dwarf corona:** The radio emission is indirectly associated with the WD in the sense that it forces the K dwarf into a rapid co-rotation enhancing stellar activity. The principal difficulty with this model is that outside eclipse one would expect the radio emission to be strongest at phase 0.5, contrary to what is actually observed.

2. **Interacting stellar magnetospheres:** Patterson et al. (1993) [54] suggested that collisional interactions between the magnetospheres of the two stars may result in the acceleration of electrons. The WD and the K-dwarf magnetic fields existence are strongly supported by the soft X-ray emission detected.

Sion et al. 1995 [59] found a lack of detectable Zeeman components in its Lyman $\alpha$ photospheric abortion. Also the order is comparable to the magnetic field from empirical relations between photospheric magnetic fluxes and rotation periods of active late-type dwarfs (Saar et al. 1987 [58]). Estimating then a $10KG$ magnetic field for the WD and K-dwarf, and assuming a dependence of this magnetic field more likely to $r^{-2}$ for the k-dwarf and $r^{-3}$ for WD, it is possible to show that the region of magnetic balance is near to the WD surface (approximately $3R_{wd}$). Figure 3.4 (Lim et. al 1996 [42]) shows the geometric picture that was theorized few years ago.

Having in mind that the accelerated charged material is transported by the K-dwarf to the WD via magnetic channeling, we can also explain in a qualitative form why one of the radio eclipsing emission seems to be stronger than the other: due to co-rotating movement of the binary star, it is possible that the particles transferred from the K-dwarf arrive more densely to one side of the WD than to the other. This leads to more material accelerated in one window of the eclipse than in the other.

### 3.2.2 Spectral Index

We can compare our recently ALMA observations of V471 Tau in the *mm* range with old VLA observations in radio. Our goal is to try to extract a parameter that can give us more evidence of magnetic origin for those emission. In fact, because our data is not able to show the polarization of the light perceived, we can use the spectral index (or at least, some conclusion about it).

The spectral index $\alpha$ of a spectral distribution is defined as:

$$S \propto \nu^{\alpha}, \tag{3.4}$$

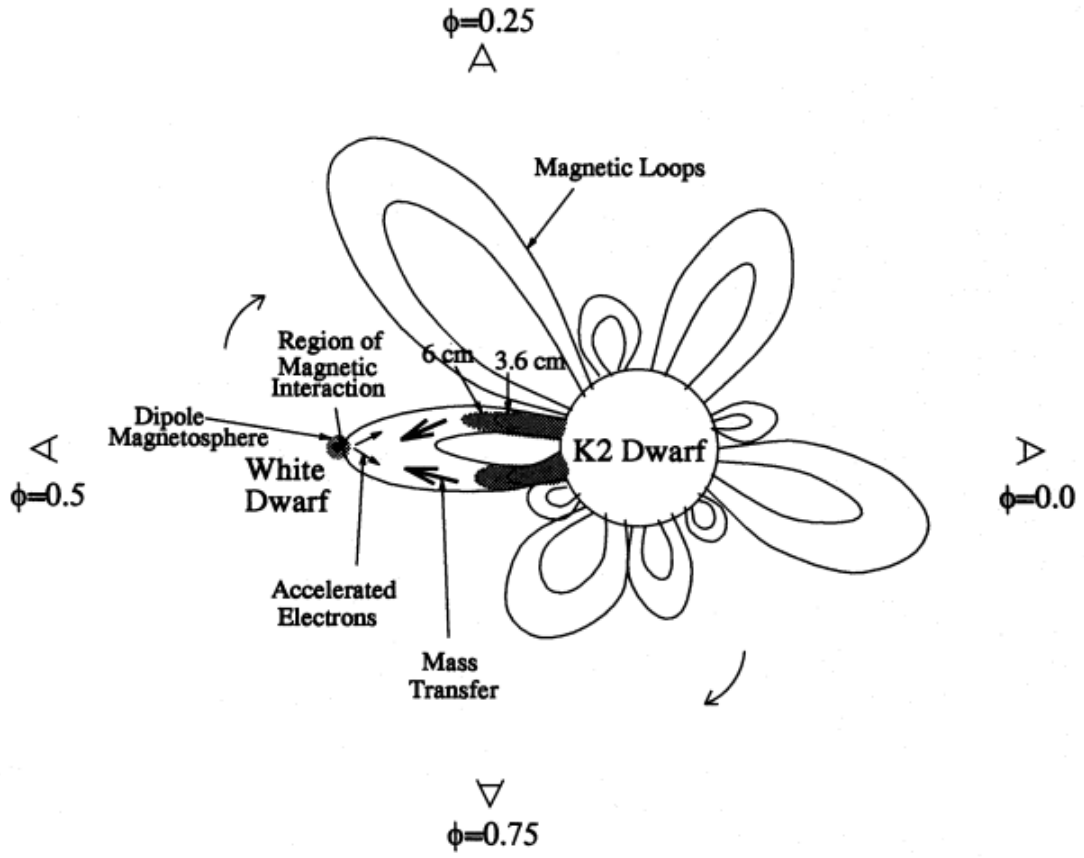


**Figure 3.4:** Geometry and mechanism for the radio and mm emission detected in V471 Tau, proposed by Lim et al. 1996 [42]

were $S$ is the flux and $\nu$ is the frequency. If we linearize the spectral distribution, $\alpha$ is simply the slope of the logarithmic linear expression:

$$\ln(S) \propto \alpha \ln(\nu) \tag{3.5}$$

It has been theorized many times how it would be the spectral shape of a synchrotron emission. In fact the shape strongly depends on the energy distribution (velocity) of the charged particles and the thickness of the source due to self-absorption processes.

If a synchrotron is optically thin ($\tau \ll 1$), then its spectrum is the superposition of the spectra from individual electrons and its flux density cannot rise faster than $\nu^{1/3}$ at any frequency $\nu$. Most astrophysical sources of synchrotron radiation have spectral indices near $\alpha \sim 0.75$ at frequencies where they are optically thin, and their high-frequency spectral indices reflect their electron energy distribution, not the spectra of individual electrons.

In a self absorption process, the spectral index tend to be 5/2, independent on the energy distribution. If the energy distribution of relativistic electrons in a synchrotron source were a (relativistic) Maxwellian distribution, the electrons would have a well-defined kinetic temperature, and synchrotron self-absorption would prevent the brightness temperature of the synchrotron radiation from exceeding the kinetic temperature of the emitting electrons. In our case, due to the density of the gas that is near both stars, the hot temperature should be considered thick, so we are looking for a spectral index similar to this value.

In Lim et. al 1996 [42], it was verified that the radio spectrum appears to be flat between 6 and 2 $cm$, but rising between 20 to 6 $cm$. If we assume that in the period 1996-2016 there was no major change in the dynamics of V471 Tau system, we can compare detections on both years and try to verify if the possible spectral index is in agreement with a synchrotron emission. Although the exact value of this parameter is impossible to extract due to the lack of more data, it is possible to do a rough estimation.

A $5/2 \sim 2.5$ spectral index implies that the linearization of our data have to follow a behaviour of a slope likely 5/2. Considering to points in the distribution as $(S_A, \nu_A)$ and $(S_B, \nu_B)$ the spectral index can be calculated as:

$$\alpha = \frac{\ln(S_B) - \ln(S_A)}{\ln(\nu_B) - \ln(\nu_A)} = \frac{\ln(S_B/S_A)}{\ln(\nu_B/\nu_A)} \tag{3.6}$$

Taking a value of $S_A = 1.2 \pm 0.1\, mJy$ at $\nu_A = 8.33 \times 10^9\, Hz$ for the 1996 data and $S_B = 2.04 \pm 0.096\, mJy$ at $\nu_B = 2.3 \times 10^{11}\, Hz$ for our observation, both in stronger emission (i.e for the window of the eclipse in which both detections reach the maximum value), let us to perform a calculation of the slope considering propagation errors as:

$$\ln(x \pm \Delta x) = \ln(x) \pm \frac{\Delta x}{x} \tag{3.7}$$

$$\frac{x + \Delta x}{y + \Delta y} = \frac{x}{y}\left(\frac{\Delta x}{x} + \frac{\Delta y}{y}\right) \tag{3.8}$$

Using the given values:

$$\ln(\nu_B/\nu_A) = \ln(2.3 \times 10^{11}/8.33 \times 10^9) = 2.7611 \tag{3.9}$$

$$\ln(S_B/S_A) = \ln(1.7 \pm 0.221) = 0.53 \pm 0.13, \tag{3.10}$$

we derive an approximated spectral index of:

$$\alpha = 0.191 \pm 0.047 \tag{3.11}$$

Lim et al. 1996 [42] stated that it is sufficient for the spectral index to be plane in order to maintain a consistent magnetic origin. The reasons behind this assumption are in Bastian, Dulk & Chanmugam et al. 1988 [6](hereafter BDC).

BDC develop a theoretical simplified framework to explain some radio emission properties in AE Aqr based on *flaring events* that occur in a relatively continuous basis. It is based in the idea of discrete injection of relativistic electrons into the system (something that is very close to our case) leading to a superposition of synchrotron sources, ignoring other possible complications like geometry or background plasma. It is interesting to cite in the paper of this year in which they compare AE Aqr with V471 Tau as follow:

*V471 Tau, a member of the Hyades, is a detached PCEB composed of a DA WD and a K2V secondary; in other words, it is a CV progenitor. Its orbital period, $\sim$ 12.5 hr, is comparable to that of AE Aqr. The K2V secondary of V471 Tau is indeed known to flare in the optical band from time to time (Young et al. 1983 [75]). It was detected on one occasion as a weak non-thermal radio source, attributed to flaring emission since the source was not detected on two previous occasions. Thus, while V471 Tau contains a K-dwarf secondary with a period comparable to that of AE Aqr and is known to flare, its radio emission is weak or nonexistent.*

These words were written as a possible argument against their theory, but now that we are sure of the radio and *mm* emission in V471 Tau, we can give extra support for the model that BDC developed.

The framework is based initially in expressions derived by Van der Laan (1966) [68](hereafter VDL) for variable extra-galactic radio sources assuming the classical electron distribution given by $n(E)dE = KE^{-\delta}dE$, where the $K$ is a constant defined by some properties of the relativistic gas. A single flare event is idealized as an impulsive injection of a spherical cloud of relativistic electrons, called a *plasmoid*, that expand adiabatically. Assuming conservation of magnetic fluxes and number of electrons and an isotropic distribution, VDL derived some expression for a single flare event $S(\nu, \rho)$ dependent on the relative radius of the plasmoid $\rho = \frac{r}{r_o}$ (see eq (2) in [6]). The important parameters for this expression are the frequency in which the emission is maximum, the optical depth at that frequency, and the initial conditions.

Using this expression, BDC were able to extract a *time averaged flux density* $\langle S(\nu, \rho) \rangle$ over the series of plasmoid doing a series of physical assumptions that are related with simplifications on the characteristic of a plasmoid. Its calculation leads to the friendly

expression as:

$$\langle S(\nu,\rho)\rangle = \nu^{\frac{5}{2}(2-\epsilon)}, \tag{3.12}$$

were $\epsilon$ is a parameter related to the frequency $f$ of flaring events with an initial peak flux density of $S_{mo}$, in which BDC assumed a simple distribution as $f(S_{mo}) = S_{mo}^{-\epsilon}$. They then suggested that many of the complex properties of the radio emission observed in AE Aqr can be understood for a model in which the emission is due to a random superposition of flaring events.

Using this expression, Abada-Simon et al. 1993 [1] were able to explain the shape of the radio spectrum observed in AE Aqr with an index $\epsilon \sim 1.8$. Interestingly, we can use the same model to explain the spectral index observed in V471 Tau. If we take the calculated value for $\alpha = 0.138 \pm 0.033$ we obtain a value for $\epsilon$ of:

$$\epsilon = 1.9236 \pm 0.0188 \tag{3.13}$$

This positive result is very important to support the idea of magnetic origin for the emission.

# Chapter 4

# Behind the origin of magnetic fields in WD

A considerable fraction of WDs in the neighborhood of the solar system show evidence of harboring strong magnetic fields, but the origin of these fields is still an open question. WDs are compact objects typically composed by Carbon and Oxygen that are in a partially or fully degenerated state, equilibrating the strong gravity with quantum pressure via Pauli exclusion principle. This lead to a high conductivity, generally isothermal distribution of temperature and high gravity pressure.

It has been shown that the relative fraction of strong magnetic fields is larger in fainter WDs (Kepler et al. 2013 [35]) which can be related with their masses (massive WDs are smaller) and/or ages (older WDs are cooler, and therefore fainter). Also, the frequency of HFMWDs in CVs is larger than in isolated WDs. However, only a few MWDs paired with detached non-degenerated companions has been found (like V471 Tau or QS Vir). The question then is: Where are the natural progenitors of CVs?

Any hypothesis that try to explain the origin of magnetic fields, needs to be consistent with three observational facts: the massiveness of MWDs, their tendency to be cold, and the non-existence of MWDs in detached binaries. The magnetic field in fact could be generated via two different mechanism: inherited from a weak magnetic field of a progenitor star, or by the evolution in a binary system. The first scenario is called *fossil field hypothesis*, in which the magnetic field is simply the consequence of

the evolution of a progenitor star (specifically Ap and Bp stars, the only class that is known for having high magnetic fields of $10^3 - 10^5$ $G$). Although is possible to show that the amplification of the magnetic field due to the shrinkage of the star is comparable with those found in MWDs, it can not explain why there are no MWDs found in detached PCEBs. The second scenario is focused in the evolution of WDs and its interaction with the companion at the binary stage. The nature of this interaction to produce the magnetic field could be theorized by many mechanism. It has been suggested that the field could be produced in the common envelope phase, due to the differential rotation that the secondary spiral-in produces in the outer layers of the convective envelope; but it has been show that this field does not penetrate in the WD and is rapidly dissipated when the material is ejected. Also, it has been shown that the field generated due differential rotation produced by the merge of two degenerated cores remains and does not decay for a very long time. However, a field produced after a merger event would not be able to explain the high fraction of MWDs among CVs, and their absence among the direct progenitors of CVs.

A new scenario was recently proposed, in which the field is generated as a consequence of the crystallization of the core of a WD as it becomes older.

## 4.1 The physics behind the crystallization theory

The theory of magnetic origin of WDs via crystallization is supported in physics very similar to the dynamo theory. In fact, when a Carbon-Oxygen (C-O) WD cools down, the Oxygen begin to precipitate to the center of the stars, because this element has a higher temperature of solidification than Carbon (Horowitz et. al 2010 [28]). The structure of the WD partially changes in the sense that is finally composed by a solid core, rich in Oxygen, surrounded by a Carbon-rich convective mantle, that was redistributed via Rayleigh-Taylor instabilities (Isern et al. 1997, 2000 [30]). The movement of this convective mantle is then the possible precursor of the magnetic field. Direct observational evidence of crystallization at the core of WDs was recently observed by Tremblay et al. (2019) [67] as a delay in the cooling sequence of WDs due to the release of latent heat as the core of the WDs crystallize.

For a deep understanding of the problem, we need to introduce ourselves in the physical processes behind the dynamo theory. Therefore, I will first introduce the concepts that we are going to use in the development of our statements. A deeper explanation can be found in Christensen et. al. 2009 [15].

### 4.1.1 Magnetohydrodinamics

The main equation of magnetohydrodinamic can be written as:

$$\rho \frac{D\mathbf{u}}{Dt} = -\nabla P - 2\rho\Omega \mathbf{e_z} \times \mathbf{u} + \rho\nu\nabla^2\mathbf{u} + \rho\alpha g T \mathbf{e_r} + \mathbf{j} \times \mathbf{B}, \tag{4.1}$$

where the left hand corresponds to the dynamic terms, and the right side takes into account the pressure, Coriolis, viscosity, buoyancy and electromagnetic forces respectively. Also, the induction equation for magnetic fields is:

$$\frac{\partial \mathbf{B}}{\partial t} = \eta\nabla^2\mathbf{B} + \nabla \times (\mathbf{u} \times \mathbf{B}), \tag{4.2}$$

where $B$ is the magnetic field, $\eta$ the magnetic diffusivity and $u$ the velocity of the fluid, related to the advection processes. This equation describes the evolution of the magnetic field according to the diffusive or advective energy expend. We can measure the predominance of one process over the other introducing the quantity called **Magnetic Reynolds Numbers** written as:

$$Rm = \frac{Lu}{\eta}, \tag{4.3}$$

where $L$ is a length scale relative to the changes of the magnetic field in the fluid.

Because of the conductive nature of WDs, the velocities of particles are large over a large scale and $Rm$ high enough; we can ignore the diffusive mechanism. In this regime,the generation and maintenance of a magnetic field due to a plasma fluid is ensured by Alfven's theorems, in which it is possible to demonstrate that the *magnetic flux linking any loop moving with the fluid is constant*.

In this way, the estimation of magnetic properties from considerations of the plasma fluid can be done assuming some balances between the present forces in Eq. 4.1.

### 4.1.2 Elsasser number rule

The first and easiest way to approach the problem, is by considering that the viscous and inertial forces are negligible due to the fluid characteristics in consideration. This allows magnetohydrodynamic equations to be studied with a primary focus on rotational and electromagnetic forces. We define the Elsasser number as a scale of the rate between the magnetic and rotational forces:

$$\Lambda = \frac{\sigma B^2}{2\rho\Omega}, \tag{4.4}$$

where $\sigma$ is the conductivity, $\rho$ the density and $\Omega$ the rotational rate.

Many studies of magnetoconvection claim that *magnetic forces have to be of an order similar to rotational forces*, because they isolated would cancel each other . This allows to develop a first scaling known as **Elsasser number rule**, in which this number must have a magnitude of the order of 1 for the sustainability of magnetic fields in stellar astrophysics. Using this rule, some definitions of classic electromagnetism, and estimations of magnetic variation scales to the size of the convective region $R_c$, we can estimate the magnetic field strength as:

$$B^2 \propto \mu_o \rho U \Omega R_c. \tag{4.5}$$

In this way, there are some methods to obtain an estimation of the field strength as a function of other parameters.

## 4.2 Scaling laws for velocity

There are different scaling laws for the fluid velocity that give us different estimations of the magnetic field generated via dynamo from a configuration, balancing all the other forces in different ways. We center our job in two of this scaling laws, because they represent the most vast application margins and allow us to obtain the more interesting results.

### 4.2.1 Mixing-Length

The mixing-length formalism corresponds to a highly turbulent fluid, in which convective transport can be created in *bubbles* of mater that travel a certain distance before they get destroyed. We can consider the balance between non-linear inertial forces and buoyancy forces, which give us the relation:

$$U \propto \left( \frac{l q_c}{\rho H_T} \right)^{\frac{1}{3}}, \tag{4.6}$$

where $q_c$ is the convective heat flux, $l$ is the mixing-length, $H_T$ temperature scale-height and $U$ is the estimated velocity of the fluid.

### 4.2.2 Mac Balance (Magnetic-Arquimedean-Coriolis)

In this model it is considered that the buoyancy forces do work against Lorentz forces, so we can balance Coriolis forces against buoyancy forces. Then we can obtain:

$$U \propto \left(\frac{q_c}{\rho\Omega H_T}\right)^{\frac{1}{2}}. \tag{4.7}$$

### 4.2.3 Magnetic field scaling based on available power

Another important point, apart from the dynamic balance of forces in the dynamo, is the thermodynamic consistency. In this sense, the ohmic dissipation associated with the field cannot exceed the available energy to be converted in other forms of this.

Stevenson (1984) [64] suggested that at high energy fluxes, the dynamo is saturated to values of $\Lambda \sim 1$. The estimated calculations made by Christensen (2006) [14] show an energy balance that takes the form:

$$\frac{B^2}{2\mu_o} \propto f_{ohm}\frac{\lambda}{U}\frac{q_c}{H_T}, \tag{4.8}$$

where $f_{ohm}$ is the available fraction of energy converted in magnetic energy and $\lambda$ is the relevant length scale, commonly assumed as $R_c$. Keeping this balance in mind and using equations (4.6) and (4.7) we can arrive two different scaling laws for the magnetic field, depending on other parameters. Respectively:

$$\frac{B^2}{2\mu_o} \propto f_{ohm}\rho^{1/3}\left(\frac{q_c\lambda}{H_T}\right)^{2/3} \tag{4.9}$$

$$\frac{B^2}{2\mu_o} \propto f_{ohm}\lambda\left(\frac{q_c\rho\Omega}{H_T}\right)^{1/2} \tag{4.10}$$

The equation (4.9) was used by Isern (2017) [29] to compute the magnetic fields in crystallized WDs. Is important to remark that the principal difference between the laws is that the first one does not depend on rotation while the second one does. The basis of the use of this law is its success to explain the magnetic fields of planets and its physical similarity with WDs (solid core surrounded by a convective liquid envelope). However, the calculations allow to explain at most magnetic fields from 0.1 MG to 1 MG. Our objective is to elucidate a mechanism to estimate, from this basis, a higher value for magnetic fields using the (4.10) scaling law as support.

## 4.3 Scaling rates

The foundation of our job is simple: with the objective of comparing the two scaling laws presented, we perform a division (rate) between both. If we consider that both laws use the same proportionality factor with respect to the WDs distribution and ensuring the same unities in both of them, we obtain the $X$ factor:

$$X = \left(\frac{\lambda^2 \rho H_T}{q_c}\right)^{1/6} \Omega^{1/2}, \tag{4.11}$$

which represents the ratio between the field strengths given by (4.9) and (4.10) scaling laws. We will use the approximation made by Isern (2017) [29] in which $H_T \sim \lambda$ and, because the WDs are relatively isothermal, and we will estimate the height-scale temperature as $H_T \sim R$, where $R$ is the radius of the WD. Also, considering that $q_c$ is the convective heat flux and the size of the external layer of convection is near to the external layer of the WD, we can estimate:

$$q_c = \frac{L}{4\pi R^2}, \tag{4.12}$$

$$\rho = \frac{3M}{4\pi R^3}, \tag{4.13}$$

where $M$ and $L$ are the mass and the luminosity of the WD respectively. Even though we could consider that part of the total luminosity that emerges from the WD is not transported under convective channels, this error in the estimation would increase the obtained value for $X$ and in no case would decrease it (since strictly $q_c \leq \frac{L}{4\pi R^2}$ for conservation of energy). We have then:

$$X = \left(\frac{3MR^2}{L}\right)^{1/6} \Omega^{1/2}. \tag{4.14}$$

We can first calculate this expression for the sun, in order to calculate the result based on the parameters expressed in solar units:

$$\left(\frac{3M_\odot {R_\odot}^2}{L_\odot}\right)^{1/6} \sim 4394[s^{1/2}]. \tag{4.15}$$

If we use $M$, $L$ and $R$ in solar units, then we have:

$$X = \left(\frac{MR^2}{L}\right)^{1/6} \Omega^{1/2} 4394[s^{1/2}]. \tag{4.16}$$

We will consider the following typical parameters for a WD:

$$\begin{aligned} M &= 0.6 M_{\odot} \\ R &= 0.015 R_{\odot} \\ L &= 0.001 L_{\odot} \\ \Omega &= 2\pi/T = 0.00175 \frac{1}{[s]} \end{aligned}$$

where we have taken a rotation period $T = 1[h]$ for the WD. So, the factor $X$ takes the value of:

$$X = \left(\frac{B_2}{B_1}\right)^2 = 132,$$

If we use $T = 60[s]$ we can obtain a value of:

$$X = \left(\frac{B_2}{B_1}\right)^2 \sim 1022,$$

where $B_1$ and $B_2$ correspond to the intensity of the field derived from equations (4.9) and (4.10) respectively. This means that the magnetic field calculated with the second scaling law is approximately 1 order of magnitude larger than that calculated with the first law. There are ways to further increase the values obtained. Strictly speaking, decreasing the luminosity or increasing the mass, radius or speed of rotation of the WD would result in a stronger field. For example, it is clear that the luminosity of a WD decreases with time, which is strictly related to a lower luminosity at the crystallization time. In this sense, if we use a $L = 10^{-5}\, L_{\odot}$ and the $T = 1[h]$, we would obtain a field 16 times larger than the previous one. Other factors such as tidal couplings can be considered in binary systems.

We have shown that the estimated value for the intensity of the magnetic field depends significantly on the assumed scaling law. A scaling law that depends on rotation could yield values at least one order of magnitude larger than those calculated by a law that does not depend on it. Although this increases the value of the magnetic field, it is insufficient to explain the magnetic fields observed in CVs, which are on average $10^{1.5}\, MG$, and can even reach $100\, MG$. This means that we must investigate other possible effects, such as the effects of tidal forces.

The effects of tidal forces can be compared to those occurring on planets in the solar system: planets appear to have larger magnetic fields when their moons are

large enough to produce significant heterogeneity in the shape of their gravitational field. This heterogeneity can result in increases in the internal movement of the star, and may increase the strength of the fields. Furthermore, it should be noted that it is currently believed that external tidal forces have the ability to heat the interior of the bodies they affect, preventing their cooling. This could imply that it takes longer for the WDs in binaries to crystallize (or never to do so), which would lead to requiring a new generation hypotheses in these cases.

# CHAPTER 5

# Discussion

In this chapter I will review observational facts of MWDs in binaries and relate them to current theories for the generation of magnetic fields. In particular, I will relate my own observational results to both, previous observations of MWDs and proposed theories for magnetic field generation.

Although it is strongly possible that most of the isolated MWDs were originated from a merger during a common envelope phase, the evolutionary track that magnetic WDs in CVs have experienced has been discussed for several years in the scientific literature and remains unanswered. It is still an open question why there is no detection of magnetic WDs among detached PCEBs, while $\sim$ 20% of CVs contain a magnetic WD magnetic according to SDSS surveys (Ferrario et al. 2015 [18]) and even up to $\sim$ 33% in a recent volume-limited sample (Pala et al. 2020 [51]). The estimated fraction of isolated MWD is $\sim$ 5% in magnitude-limited samples and it increases to $\sim 10 - 20\%$ in volume-limited samples (e.g., Kepler et al. 2013 [35]).

CVs are compact binary stars that have a non-degenerate companion filling the Roche lobe and transferring material to the degenerate one. Magnetic CVs are commonly classified as *Polars* if they are highly magnetic and synchronized, or *Intermediate Polars* (IP) if the field is not high enough to synchronize the WD spin period with the binary one.

There is strong evidence of cold and therefore old MWDs in detached systems, but MWDs are completely absent in younger (hotter) PCEBs. If a dynamo generated

| $M_{WD}$ | $\log(L[L_\odot])$ | $\log(T_{eff}[K])$ | $T_{cool}[Gyr]$ |
|---|---|---|---|
| 1.30 | -1.60404 | 4.54179 | 0.14 |
| 1.25 | -1.86522 | 4.44118 | 0.23 |
| 1.20 | -2.06615 | 4.36377 | 0.31 |
| 1.15 | -2.25727 | 4.29375 | 0.41 |
| 1.10 | -2.41488 | 4.23535 | 0.50 |
| 1.05 | -2.56341 | 4.18137 | 0.61 |
| 1.00 | -2.68652 | 4.13538 | 0.70 |
| 0.95 | -2.84481 | 4.08191 | 0.85 |
| 0.90 | -2.97175 | 4.03725 | 0.99 |
| 0.80 | -3.22557 | 3.94978 | 1.33 |
| 0.70 | -3.48046 | 3.86357 | 1.77 |
| 0.60 | -3.74014 | 3.77727 | 2.35 |
| 0.50 | -3.87219 | 3.72342 | 2.81 |
| 0.40 | -3.98130 | 3.67464 | 3.46 |

**Table 5.1:** Luminosity, effective temperature and cooling age at the onset of core-crystallization for WDs with different masses from Tremblay et al. 2019 [67]

via common envelope in compact binary star results in a strongly magnetic field, we should be able to find MWDs in a large amount of PCEBS (Belloni et al. 2020 [7]). But, as mentioned above, we only find cold MWDs in close detached binaries. These detached systems were initially termed *low accretion rate polars* (LARPs) but later considered to be rather progenitors of polars (*pre-polars*). These detached binaries are old and cold, are almost filling the Roche lobe, and the WD is accreting from the wind of the secondary at a very low rate. The observational fact that young detached binaries with MWDs do not exist, implies that mechanisms that generate the magnetic field during common envelope evolution are unable to reproduce the observations.

Crystallization seems to be a strong alternative to solve this problem as it introduces a time-dependence to the magnetic field generation. The effective temperature at the onset of crystallization strongly depends on the mass of the WD (Tremblay et al. 2019 [67]). Table 5 gives the luminosity, effective temperature and age at which the core of a WD begins to crystallize, for different WD masses. We used the luminosity versus effective temperature at the onset of crystallization from Tremblay et al.

2019 [67], combined with the cooling models from Fontaine et al. (2001) [22] to obtain the corresponding WD mass and cooling age. It is evident that the process is much faster for the more massive WDs, which crystallize at a higher temperature. As helium does not crystallize under the physical conditions present in a WD, this scenario would naturally explain the higher fraction of HFMWDs among CVs, as helium-core WDs are absent among them (Zorotovic et al. 2011 [77]). The observed differences would also arise from the current observational limitation of detecting low temperature WDs, among single WDs but especially if they are overshadowed by a companion in a detached binary system. In the case of CVs, on the other hand, we would be able to detect many of them, because accretion increases their luminosities and compressional heating increases the WD surface temperature.

This model has his own pros and cons, as I will discuss in what follows focused on different populations of WDs.

## 5.1 Single MWDs

1. There are some isolated WDs with fields exceeding 100 MG, which seem hard to be explained within the crystallization scenario with our current knowledge of the dynamo generated.

2. There are also MWDs that are known to be slow rotators (with periods of years) showing evidence for extremely large magnetic fields. For a rotational period of $\sim$ 1 yr, we obtain from Eq. 4.3 (and keeping all other assumptions for the WD) a field of the same order of magnitude as the one derived by Isern et al. (2017) [29]. We do not know if another scaling law, better suited for WDs, could yield such high field strengths even in the absence of rapid rotation.

3. It is evident that crystallization can not explain the magnetic fields observed in all single WDs, because many hot single magnetic WDs (above the temperature limit for crystallization) do exist.

In summary, the crystallization scenario could explain the fields detected in some of the single WDs, but a different origin is needed for most of them, especially for hot MWDs (above the crystallization limit), for HFMWDs with long rotational periods, and for those with very strong fields.

## 5.2 Detached WD+MS binaries and pre-CVs

1. For the population of detached WD plus main-sequence binaries, i.e. the CV progenitors, the crystallization scenario predicts that a not negligible fraction of MWDs should exist among them, but they would be almost completely hidden from us because of the observational limitation in detecting a cold WD against a MS companion in the absence of mass transfer. Moreover, Camacho et al. (2014) [13] found that the PCEB sample from SDSS is strongly biased against the detection of massive WDs, i.e. the ones that begin the crystallization process faster. Therefore, if core- crystallization were able to produce many MWDs in detached WD+MS systems, a strong observational bias against their identification could explain the lack of observed MWDs among detached WD+MS binaries from SDSS.

2. The low temperature of the WDs in pre-polars (or LARPs) can be naturally explained by the crystallization process, since only sufficiently cool WDs can develop a significant magnetic field.

In the case of LARPs, it is strongly possible that all of them are highly magnetic due to crystallization processes. However, the scaling laws used in Isern et al. 2017 [29] and here, need a high rotation period for the WD ($\sim 60\,s$) to increase the strength of the field developed. A good explanation for this is that maybe all the LARPs were CVs before. It has been studied in the literature that mass transfer in a CV increases the angular momentum of the WD (King et al. 1991) [38]. Furthermore, Hameury et al. 1987 [26] showed that a strong magnetic field will lead to synchronisation of the orbital period and the WD spin period, causing the binary star to increase its separation. The following scenario appears possible: mass transfer in CVs increases the angular momentum and rotation of the WD and, at some point, the WD crystallises and the dynamo in the WD's convective mantle generates a magnetic field. Then the system detaches due to synchronisation and we observe the systems as LARPs.

### 5.2.1 Confronting the crystallisation dynamo with observations of PCEBs

It is interesting to confront our hypothesis with the systems we observed and other presented in the literature. For this purpose it is very useful to use table 5. The table

shows the distribution of WD mass and effective temperature for different measured values.

### NN Ser

The NN Ser detections are particulary special. As we discuss in the previous sections, it is completely safe to state that we can discard the cold dust hypothesis, although it seems that the *mm* detections does not match with a megaflare due to comparison to others red dwarf stars. Moreover, if we call arguments that could increase the magnetic activity of the red dwarf star, the enormous difference in order of magnitude does not give us a strong evidence of this kind of process happening in the star. It seems to be more likely a false positive in the second detection.

### V471 Tau

V471 Tau was found to be a magnetic PCEB system with a highly radio emission due to magnetic processes. Although in the literature it has been estimated a field of the order of $0.01MG$ (Lim et al. 2996 [42], we cannot estimate a clear value for the magnetic field of the WD, but we can theoretically work with the idea of V471 Tau being a magnetic star by the evidence presented before and in this thesis, and try to elucidate its evolution track.

Crystallization can predict values up to $1 - 10MG$. Altought V471 Tau seems to be a moderate magnetic star, it cannot be explained by crystallizatio as it is too young and hot to crystallize (O'Brien et al. 2001 [48]).

We tend to state that V471 Tau is more likely a post merger system. Some indications are:

1. V471 Tau is a member of Hyades cluster and it has the youngest star.
2. It is also the most massive of them and the hottest, with a temperature of $T = 34\,500 \pm 1\,000K$

According to O'brien et al. 2001 [48], a possible scenario is that the progenitor system was a triple, with a close inner pair of main-sequence stars. These stars became an Algol-type binary, which merged after several hundred million years to produce a single blue straggler of about twice the turnoff mass. When this star evolved to the AGB phase, it underwent a common-envelope interaction with a more-distant dK companion, which spiralled down to its present separation, and ejected the envelope.

Also, the merger hypothesis explains the magnetic processes happening in the star without call the crystallization theory, fossil-field or other processes.

### QS Vir

QS Vir is another interesting PCEB composed by a WD and a M Dwarf star discussed amply by researchers. The M star's radius is still within its Roche lobe and there is no evidence that it is over-inflated. We have ALMA data for this star giving positive detection, but the details of this could not be included in this thesis and will be subject of study in the future.

Ignoring that, there is strong evidence in the literature about the magnetic activity of this star (Parsons et. al 2016 [52]). Altought it is very difficult to state what is the correct evolutionary track behind this binary star, we can theorize if crystallization can give a explanation for its behaviour considering the principal characteristics of QS Vir.

1. O'Donoghue et al. (2003) [49] suggested that QS Vir is a hibernating CV.

2. Its orbital period is 3.618 hrs (Almeida et al. 2010)

3. The temperature of the WD is $14\,220 \pm 350K$ and is relatively massive, $0.782 \pm 0.013 M_{\odot}$ (Parsons et al. 2016 [52])

However, if we see table 5, the WD in QS Vir is locate above the limit for crystallized WDs. This suggest that there are others processes happening in this star that can increase the magnetic activity. The tidal forces that the red dwarf star performs into the WD could be and effect to consider. It has been studied in the earth that the moon could be a strong source of energy to generate and maintain the magnetic field of the earth, due to failure in older models that do not consider this issue (Andrault et al. 2016 [3]). The theory is that tidal distortions of a planet induced by gravitational interactions with a companion (e.g. Earth and Moon) are both capable of generating core turbulence. A rotating fluid, permit eigenmodes of oscillation called "inertial modes", whose restoring force is the Coriolis force. Precession and tides can resonate exciting those inertial modes, leading to fluid instabilities, turbulence and dynamo action. In either case, it is important to recognize that a resonance is involved: even if the excitation amplitude is small, the resulting flows may be intense, draining their energy from the mechanism sustaining the excited waves, i.e. from the spin–orbit rotational energy of the considered system. Thinking in QS Vir as a binary star rotating very fast

and extremely near one body to each other, it is possible that tidal forces and its contribution to the generation of magnetic field would be an interesting research topic for the future.

## 5.3 Crystallization and CVs

Some parameters to consider in the development of magnetic fields are:

1. **Mass:** Zorotovic et al. (2011)[77] showed the WD mass distribution for CVs is different from that observed in detached WD+dM binaries, which have a lower average WD mass ($\sim 0.6 M_{\odot}$) than WDs in CVs ($0.83 M_{\odot}$), in which helium-core WDs are absent (Rebassa-Mansergas et al. 2011 [56]). Schreiber et al. (2016) [61] suggested that systems with low-mass WDs are more likely to suffer a merge, caused by novae eruptions, shortly after the beginning of the CV phase. As massive WDs do also exist in detached WD+dM binaries, if the WD mass were the only parameter that determines the probability of developing a high magnetic field, we should see a not negligible percentage of strongly magnetized WDs among detached WD+dM systems, which is not observed.

2. **Age:** The WDs in CVs should be older than their detached progenitors. This does not necessarily imply that they are colder, because CVs are dominated by high-mass WDs that cool slowly. However, there is an observational bias against the detection of detached systems with cool WDs, as these can be completely overshadowed by their MS companions. CVs would not be affected (or at least should be less affected) by this bias, because the effects of mass transfer make it possible to detect CVs with cooler WDs.

Then, the evidence in both single WDs and WDs in binary stars suggests that the incidence of WDs with strong magnetic fields increases for the more massive and older WDs, which are parameters that are related with crystallization. Also, both features (massive and older) are presented in CVs. Moreover the absence of helium-core WDs (which are not expected to be crystallized) in those stars is another argument to support this theory.

IPs and polars are CVs with strong magnetic fields. Polars are different to IPs only in the fact that they are more strongly magnetic and because of that, they are synchronized. The origin of the magnetic fields is discussed along the literature and clear

answers have not been given yet, meaning that maybe more than one explanation for the origin is needed. Polars are usually synchronised systems and their WD magnetic fields are of the order of 10 - 100 MG, which is strong enough to prevent the formation of an accretion disc. WDs in IPs, on the other hand, have weaker magnetic fields ($\sim$ 1 - 10 MG), which implies that most IPs are asynchronous systems that possess truncated accretion discs.

With our calculation using models in chapter 4, we can state that the field predicted by crystallization can increase one order of magnitude using a different scaling law. Although it could be possible to explain IPs, it is not able to explain the extremely strong fields in polars. Here we can think again in tidal effects to increase the values of the magnetic fields in those kind of stars. Thus, in order to have core-crystallization as a viable channel to explain magnetic CV properties, a better understanding of the dynamo process in crystallized WDs is needed to evaluate under which conditions the field strength of polars and IPs, as well as their orbital period distributions, could be explained. It is possible also that HFMWDs in CVs have a fossil field origin, because a large fraction of WDs in CVs descend from very massive progenitors, or even that we need a different scaling law with special considerations to the nature of the degenerate and compact stars.

# Chapter 6

# Conclusions

Crystallization seems to be a promising theory that, with other mechanism, as mergers or fossil-field generation, can help to elucidate the evolution and the origin of most of the MWDs present in the Universe, isolated or not. We can give a summary and comparative table to see how some of the different MWDs can be explained and their possible origin. We are emphatic to point out that it is very possible to have more than one mechanism to explain each case.

Also we studied here a particular case of a magnetic process happening in a PCEB star that seems to be moderate magnetic: V471 Tau. Although the mass transfer has not been detected in this system, we studied a secondary signal coming probably from charges accelerated due to interacting magnetospheres that give us good information about the magnetism in this star. This could be a strong tool to study other magnetic PCEBs like QS Vir in the future, and help to elucidate the evolution of MWDs in general.

| Type of MWD | Possible and most convincing explanation | Main Reasons |
|---|---|---|
| Isolated MWDs | Merger process | - High mass<br>- Some fields exceeding 100 MG<br>- Some are slow rotators<br>- $\sim$ 62 per cent of the single magnetic WDs from the Montreal WD Database are above the crystallization limit |
| Detached MWDs | Understandable | - Strong observational bias against the detection of systems with cold WDs<br>- The sample is dominated by systems with WD masses below $\sim 0.6 - 0.7 M_{\odot}$, for which the crystallization time is longer<br>- Descend from less massive progenitors than required for the fossil field scenario to work<br>- The merger scenarios, either during a common-envelope phase or in a double WD binary system would only be possible for a small fraction of wide binary systems in which the inner binary in an originally triple system experienced a merge |
| LARPs (Pre-polars) | Crystallization | - Low temperature and high mass<br>- Detected because of mass transfer<br>- Possible CV past that creates the magnetic field present now |
| Intermediate Polars | Crystallization | - The calculations give a good value to explain those magnetic fields |
| Polars | Fossil-Field | - Enormous magnetic fields<br>- Very high mass WDs descend from very massive objects |

# Bibliography


[1] Meil Abada-Simon, Alain Lecacheux, Tim S. Bastian, Jay A. Bookbinder, and George A. Dulk. The Spectrum and Variability of Radio Emission from AE Aquarii. ApJ, 406:692, April 1993.

[2] B. P. Abbott, R. Abbott, T. D. Abbott, et al., LIGO Scientific Collaboration, and Virgo Collaboration. GW170817: Observation of Gravitational Waves from a Binary Neutron Star Inspiral. Phys. Rev. Lett., 119(16):161101, October 2017.

[3] Denis Andrault, Julien Monteux, Michael Le Bars, and Henri Samuel. The deep Earth may not be cooling down. *Earth and Planetary Science Letters*, 443:195–203, June 2016.

[4] J. R. P. Angel, E. F. Borra, and J. D. Landstreet. The magnetic fields of white dwarfs. ApJS, 45:457–474, March 1981.

[5] M. Aurière, G. A. Wade, J. Silvester, F. Lignières, S. Bagnulo, K. Bale, B. Dintrans, J. F. Donati, C. P. Folsom, M. Gruberbauer, A. Hui Bon Hoa, S. Jeffers, N. Johnson, J. D. Landstreet, A. Lèbre, T. Lueftinger, S. Marsden, D. Mouillet, S. Naseri, F. Paletou, P. Petit, J. Power, F. Rincon, S. Strasser, and N. Toqué. Weak magnetic fields in Ap/Bp stars. Evidence for a dipole field lower limit and a tentative interpretation of the magnetic dichotomy. A&A, 475(3):1053–1065, December 2007.

[6] T. S. Bastian, G. A. Dulk, and G. Chanmugam. Radio Flares from AE Aquarii: A Low-Power Analog to Cygnus X-3? ApJ, 324:431, January 1988.

[7] Diogo Belloni and Matthias R. Schreiber. Are white dwarf magnetic fields in close binaries generated during common-envelope evolution? MNRAS, 492(1):1523–1529, February 2020.

[8] K. Beuermann, F. V. Hessman, S. Dreizler, T. R. Marsh, S. G. Parsons, D. E. Winget, G. F. Miller, M. R. Schreiber, W. Kley, V. S. Dhillon, S. P. Littlefair, C. M. Copper-

wheat, and J. J. Hermes. Two planets orbiting the recently formed post-common envelope binary NN Serpentis. A&A, 521:L60, October 2010.

[9] P. M. S. Blackett. The Magnetic Field of Massive Rotating Bodies. Nature, 159(4046):658–666, May 1947.

[10] Jonathan Braithwaite and Hendrik C. Spruit. A fossil origin for the magnetic field in A stars and white dwarfs. Nature, 431(7010):819–821, October 2004.

[11] Gordon P. Briggs, Lilia Ferrario, Christopher A. Tout, and Dayal T. Wickramasinghe. Origin of magnetic fields in cataclysmic variables. MNRAS, 481(3):3604–3617, December 2018.

[12] Carolyn Brinkworth. Testing the first direct measurement of cataclysmic variable evolution: the search for a circumbinary disk or a low?mass companion around NN Serpentis. HST Proposal, July 2006.

[13] Judit Camacho, Santiago Torres, Enrique García-Berro, Mónica Zorotovic, Matthias R. Schreiber, Alberto Rebassa-Mansergas, Ada Nebot Gómez-Morán, and Boris T. Gänsicke. Monte Carlo simulations of post-common-envelope white dwarf + main sequence binaries: comparison with the SDSS DR7 observed sample. A&A, 566:A86, June 2014.

[14] U. R. Christensen and J. Aubert. Scaling properties of convection-driven dynamos in rotating spherical shells and application to planetary magnetic fields. *Geophysical Journal International*, 166(1):97–114, July 2006.

[15] Ulrich R. Christensen, Volkmar Holzwarth, and Ansgar Reiners. Energy flux determines magnetic field strength of planets and stars. Nature, 457(7226):167–169, January 2009.

[16] Jeffrey Cummings, Jason Curtis, Jason Kalirai, Pier-Emmanuel Tremblay, Pierre Bergeron, and Enrico Ramirez-Ruiz. The Non-Linear Initial-Final Mass Relation for Stars from 0.8 to 2.8 Msun. In *American Astronomical Society Meeting Abstracts #233*, volume 233 of *American Astronomical Society Meeting Abstracts*, page 341.03, January 2019.

[17] L. Ferrario, D. T. Wickramasinghe, and G. D. Schmidt. Modelling of Low-Accretion Rate Polars. In J. M. Hameury and J. P. Lasota, editors, *The Astrophysics*

*of Cataclysmic Variables and Related Objects*, volume 330 of *Astronomical Society of the Pacific Conference Series*, page 411, August 2005.

[18] Lilia Ferrario, Domitilla de Martino, and Boris T. Gänsicke. Magnetic White Dwarfs. Space Sci. Rev., 191(1-4):111–169, October 2015.

[19] Lilia Ferrario and Rainer Wehrse. Accretion funnels in AM Herculis systems - I. Model characteristics. MNRAS, 310(1):189–202, November 1999.

[20] Lilia Ferrario, Dayal Wickramasinghe, and Adela Kawka. Magnetic fields in isolated and interacting white dwarfs. *Advances in Space Research*, 66(5):1025–1056, September 2020.

[21] A. V. Filippenko and A. G. Riess. Results from the High-z Supernova Search Team. Phys. Rep., 307:31–44, December 1998.

[22] G. Fontaine. White Dwarf Stars as Cosmochronometers. In Ted von Hippel, Chris Simpson, and Nadine Manset, editors, *Astrophysical Ages and Times Scales*, volume 245 of *Astronomical Society of the Pacific Conference Series*, page 173, January 2001.

[23] L. A. Fowler, J. M. Cordes, and J. H. Taylor. Progress report on the binary pulsar 1913+16. *Australian Journal of Physics*, 32:35–41, March 1979.

[24] Enrique García-Berro, Pablo Lorén-Aguilar, Gabriela Aznar-Siguán, Santiago Torres, Judit Camacho, Leandro G. Althaus, Alejand ro H. Córsico, Baybars Külebi, and Jordi Isern. Double Degenerate Mergers as Progenitors of High-field Magnetic White Dwarfs. ApJ, 749(1):25, April 2012.

[25] N. Giammichele, P. Bergeron, and P. Dufour. Know Your Neighborhood: A Detailed Model Atmosphere Analysis of Nearby White Dwarfs. ApJS, 199(2):29, April 2012.

[26] J. M. Hameury, A. R. King, J. P. Lasota, and H. Ritter. The Evolution of Magnetic Cataclysmic Variables. ApJ, 316:275, May 1987.

[27] Adam Hardy, Matthias R. Schreiber, Steven G. Parsons, Claudio Caceres, Carolyn Brinkworth, Dimitri Veras, Boris T. Gänsicke, Thomas R. Marsh, and Lucas Cieza. The detection of dust around NN Ser. MNRAS, 459(4):4518–4526, July 2016.

[28] C. J. Horowitz, A. S. Schneider, and D. K. Berry. Crystallization of Carbon-Oxygen Mixtures in White Dwarf Stars. Phys. Rev. Lett., 104(23):231101, June 2010.

[29] J. Isern, E. García-Berro, B. Külebi, and P. Lorén-Aguilar. Magnetic Fields and the Crystallization of White Dwarfs. In P. E. Tremblay, B. Gaensicke, and T. Marsh, editors, *20th European White Dwarf Workshop*, volume 509 of *Astronomical Society of the Pacific Conference Series*, page 409, March 2017.

[30] J. Isern, R. Mochkovitch, E. García-Berro, and M. Hernanz. The Physics of Crystallizing White Dwarfs. ApJ, 485(1):308–312, August 1997.

[31] K. A. Jensen, J. H. Swank, R. Petre, E. F. Guinan, E. M. Sion, and H. L. Shipman. EXOSAT Observations of V471 Tauri: A 9.25 Minute White Dwarf Pulsation and Orbital Phase Dependent X-Ray Dips. ApJ, 309:L27, October 1986.

[32] A. Kawka and S. Vennes. Ap stars as progenitors of magnetic white dwarfs. In Juraj Zverko, Jozef Ziznovsky, Saul J. Adelman, and Werner W. Weiss, editors, *The A-Star Puzzle*, volume 224 of *IAU Symposium*, pages 879–885, December 2004.

[33] Adela Kawka and Stephane Vennes. White Dwarfs in the GALEX survey. In *UV Astronomy: Stars from Birth to Death*, pages 237–242, July 2007.

[34] James C. Kemp. Quantum-Magnetic Features in the Polarized Light of Grw+70°8247. ApJ, 162:L69, October 1970.

[35] S. O. Kepler, I. Pelisoli, S. Jordan, S. J. Kleinman, D. Koester, B. Külebi, V. Peçanha, B. G. Castanheira, A. Nitta, J. E. S. Costa, D. E. Winget, A. Kanaan, and L. Fraga. Magnetic white dwarf stars in the Sloan Digital Sky Survey. MNRAS, 429(4):2934–2944, March 2013.

[36] Mukremin Kilic, P. Bergeron, Alekzander Kosakowski, Warren R. Brown, Marcel A. Agüeros, and Simon Blouin. The 100 pc White Dwarf Sample in the SDSS Footprint. ApJ, 898(1):84, July 2020.

[37] D. Kilkenny, D. O'Donoghue, and R. S. Stobie. First results from thee Edinburgh-Caoe faint blue objectsurvey - normal stars at high galactic latitudes. MNRAS, 248:664–669, February 1991.

[38] Andrew R. King and Jean-Pierre Lasota. Spin Evolution and Magnetic Fields in Cataclysmic Variables. ApJ, 378:674, September 1991.

[39] J. D. Landstreet and S. Bagnulo. Discovery of kilogauss magnetic fields on the nearby white dwarfs WD 1105-340 and WD 2150+591. A&A, 623:A46, March 2019.

[40] Jianke Li. Magnetic bracking in single and binary stars. *Proceedings of the Astronomical Society of Australia*, 11:194–197, August 1994.

[41] James Liebert, P. Bergeron, and J. B. Holberg. The True Incidence of Magnetism Among Field White Dwarfs. AJ, 125(1):348–353, January 2003.

[42] Jeremy Lim, Stephen M. White, and Scott L. Cully. The Eclipsing Radio Emission of the Precataclysmic Binary V471 Tauri. ApJ, 461:1009, April 1996.

[43] Meredith A. MacGregor. Millimeter Studies of Nearby Debris Disks. In *American Astronomical Society Meeting Abstracts #229*, volume 229 of *American Astronomical Society Meeting Abstracts*, page 327.03, January 2017.

[44] T. R. Marsh, S. G. Parsons, M. C. P. Bours, S. P. Littlefair, C. M. Copperwheat, V. S. Dhillon, E. Breedt, C. Caceres, and M. R. Schreiber. The planets around NN Serpentis: still there. MNRAS, 437(1):475–488, January 2014.

[45] Jack McCleery, Pier-Emmanuel Tremblay, Nicola Pietro Gentile Fusillo, Mark A. Hollands, Boris T. Gänsicke, Paula Izquierdo, Silvia Toonen, Tim Cunningham, and Alberto Rebassa-Mansergas. Gaiawhite dwarfs within 40 pc II: the volume-limited northern hemisphere sample. MNRAS, July 2020.

[46] A. Nebot Gómez-Morán, A. D. Schwope, M. R. Schreiber, and B. T. Gänsicke. SDSS121258.25-012310.1: A new eclipsing post common envelope binary. In *Journal of Physics Conference Series*, volume 172 of *Journal of Physics Conference Series*, page 012027, June 2009.

[47] J. Nordhaus, S. Wellons, D. S. Spiegel, B. D. Metzger, and E. G. Blackman. Formation of high-field magnetic white dwarfs from common envelopes. *Proceedings of the National Academy of Science*, 108(8):3135–3140, February 2011.

[48] M. Sean O'Brien, Howard E. Bond, and Edward M. Sion. Hubble Space Telescope Spectroscopy of V471 Tauri: Oversized K Star, Paradoxical White Dwarf. ApJ, 563(2):971–986, December 2001.

[49] D. O'Donoghue, C. Koen, D. Kilkenny, R. S. Stobie, D. Koester, M. S. Bessell, N. Hambly, and H. MacGillivray. The DA+dMe eclipsing binary EC13471-1258: its cup runneth over ... just. MNRAS, 345(2):506–528, October 2003.

[50] B. Paczynski. Common Envelope Binaries. In Peter Eggleton, Simon Mitton, and John Whelan, editors, *Structure and Evolution of Close Binary Systems*, volume 73 of *IAU Symposium*, page 75, January 1976.

[51] A. F. Pala, B. T. Gänsicke, E. Breedt, C. Knigge, J. J. Hermes, N. P. Gentile Fusillo, M. A. Holland s, T. Naylor, I. Pelisoli, M. R. Schreiber, S. Toonen, A. Aungwerojwit, E. Cukanovaite, E. Dennihy, C. J. Manser, M. L. Pretorius, S. Scaringi, and O. Toloza. A Volume-limited Sample of Cataclysmic Variables from Gaia DR2: Space Density and Population Properties. MNRAS, 494(3):3799–3827, April 2020.

[52] S. G. Parsons, C. A. Hill, T. R. Marsh, B. T. Gänsicke, C. A. Watson, D. Steeghs, V. S. Dhillon, S. P. Littlefair, C. M. Copperwheat, M. R. Schreiber, and M. Zorotovic. The crowded magnetosphere of the post-common-envelope binary QS Virginis. MNRAS, 458(3):2793–2812, May 2016.

[53] S. G. Parsons, T. R. Marsh, C. M. Copperwheat, V. S. Dhillon, S. P. Littlefair, R. D. G. Hickman, P. F. L. Maxted, B. T. Gänsicke, E. Unda-Sanzana, J. P. Colque, N. Barraza, N. Sánchez, and L. A. G. Monard. Orbital period variations in eclipsing post-common-envelope binaries. MNRAS, 407(4):2362–2382, October 2010.

[54] Joseph Patterson, Jean-Pierre Caillault, and David R. Skillman. Radio Light Curves of V471 Tauri. PASP, 105:848, August 1993.

[55] Saul Perlmutter, Michael S. Turner, and Martin White. Constraining Dark Energy with Type Ia Supernovae and Large-Scale Structure. Phys. Rev. Lett., 83(4):670–673, July 1999.

[56] A. Rebassa-Mansergas, M. R. Schreiber, B. T. Gänsicke, A. Nebot Gómez-Morán, and J. Girven. The Primary Mass Distribution of PCEBs. In L. Schmidtobreick, M. R. Schreiber, and C. Tappert, editors, *Evolution of Compact Binaries*, volume 447 of *Astronomical Society of the Pacific Conference Series*, page 183, September 2011.

[57] E. Regös and C. A. Tout. *Formation of CVs by Magnetic Fields in Common-Envelopes*, volume 205 of *Astrophysics and Space Science Library*, page 424. 1995.

[58] Steven H. Saar and C. J. Schrijver. *Empirical Relations Between Magnetic Fluxes and Atmospheric Radiative Losses for Cool Dwarf Stars*, volume 291, pages 38–40. 1987.

[59] K. G. Schaefer, H. E. Bond, R. A. Saffer, and E. M. Sion. HST Observations of the White Dwarf in V471 Tauri. In *American Astronomical Society Meeting Abstracts*,

volume 187 of *American Astronomical Society Meeting Abstracts*, page 18.04, December 1995.

[60] M. R. Schreiber and B. T. Gänsicke. The age, life expectancy, and space density of Post Common Envelope Binaries. A&A, 406:305–321, July 2003.

[61] M. R. Schreiber, M. Zorotovic, and T. P. G. Wijnen. Three in one go: consequential angular momentum loss can solve major problems of CV evolution. MNRAS, 455(1):L16–L20, January 2016.

[62] Edward M. Sion and Warren Sparks. On the Effect of Explosive Thermonuclear Burning on the Accreted Envelopes of White Dwarfs in Cataclysmic Variables. ApJ, 796(1):L10, November 2014.

[63] S. J. Smartt, J. J. Eldridge, R. M. Crockett, and J. R. Maund. The death of massive stars - I. Observational constraints on the progenitors of Type II-P supernovae. MNRAS, 395(3):1409–1437, May 2009.

[64] D. J. Stevenson. The Energy Flux Number and Three Types of Planetary Dynamo. *Astronomische Nachrichten*, 305:257, January 1984.

[65] K. D. Temmink, S. Toonen, E. Zapartas, S. Justham, and B. T. Gänsicke. Looks can be deceiving. Underestimating the age of single white dwarfs due to binary mergers. A&A, 636:A31, April 2020.

[66] C. A. Tout, D. T. Wickramasinghe, J. Liebert, L. Ferrario, and J. E. Pringle. Binary star origin of high field magnetic white dwarfs. MNRAS, 387(2):897–901, June 2008.

[67] Pier-Emmanuel Tremblay, Gilles Fontaine, Nicola Pietro Gentile Fusillo, Bart H. Dunlap, Boris T. Gänsicke, Mark A. Hollands, J. J. Hermes, Thomas R. Marsh, Elena Cukanovaite, and Tim Cunningham. Core crystallization and pile-up in the cooling sequence of evolving white dwarfs. Nature, 565(7738):202–205, January 2019.

[68] H. van der Laan. A Model for Variable Extragalactic Radio Sources. Nature, 211(5054):1131–1133, September 1966.

[69] H. M. van Horn. Crystallization of White Dwarfs. ApJ, 151:227, January 1968.

[70] S. Vennes and A. Kawka. The Core Composition of a White Dwarf in a Close Double-degenerate System. ApJ, 745(1):L12, January 2012.

[71] R. F. Webbink and D. T. Wickramasinghe. A Model for Low Accretion Rate Polars. In J. M. Hameury and J. P. Lasota, editors, *The Astrophysics of Cataclysmic Variables and Related Objects*, volume 330 of *Astronomical Society of the Pacific Conference Series*, page 137, August 2005.

[72] Dayal T. Wickramasinghe, Christopher A. Tout, and Lilia Ferrario. The most magnetic stars. MNRAS, 437(1):675–681, January 2014.

[73] L. Wisotzki, W. Wamstecker, and D. L. Reimers. Discovery of a new bright southern QSO. A&A, 247:L17, July 1991.

[74] Donald G. York, J. Adelman, Jr. Anderson, John E., Scott F. Anderson, James Annis, Neta A. Bahcall, J. A. Bakken, Robert Barkhouser, Steven Bastian, Eileen Berman, William N. Boroski, Steve Bracker, Charlie Briegel, John W. Briggs, J. Brinkmann, Robert Brunner, Scott Burles, Larry Carey, Michael A. Carr, Francisco J. Castander, Bing Chen, Patrick L. Colestock, A. J. Connolly, J. H. Crocker, István Csabai, Paul C. Czarapata, John Eric Davis, Mamoru Doi, Tom Dombeck, Daniel Eisenstein, Nancy Ellman, Brian R. Elms, Michael L. Evans, Xiaohui Fan, Glenn R. Federwitz, Larry Fiscelli, Scott Friedman, Joshua A. Frieman, Masataka Fukugita, Bruce Gillespie, James E. Gunn, Vijay K. Gurbani, Ernst de Haas, Merle Haldeman, Frederick H. Harris, J. Hayes, Timothy M. Heckman, G. S. Hennessy, Robert B. Hindsley, Scott Holm, Donald J. Holmgren, Chi-hao Huang, Charles Hull, Don Husby, Shin-Ichi Ichikawa, Takashi Ichikawa, Željko Ivezić, Stephen Kent, Rita S. J. Kim, E. Kinney, Mark Klaene, A. N. Kleinman, S. Kleinman, G. R. Knapp, John Korienek, Richard G. Kron, Peter Z. Kunszt, D. Q. Lamb, B. Lee, R. French Leger, Siriluk Limmongkol, Carl Lindenmeyer, Daniel C. Long, Craig Loomis, Jon Loveday, Rich Lucinio, Robert H. Lupton, Bryan MacKinnon, Edward J. Mannery, P. M. Mantsch, Bruce Margon, Peregrine McGehee, Timothy A. McKay, Avery Meiksin, Aronne Merelli, David G. Monet, Jeffrey A. Munn, Vijay K. Narayanan, Thomas Nash, Eric Neilsen, Rich Neswold, Heidi Jo Newberg, R. C. Nichol, Tom Nicinski, Mario Nonino, Norio Okada, Sadanori Okamura, Jeremiah P. Ostriker, Russell Owen, A. George Pauls, John Peoples, R. L. Peterson, Donald Petravick, Jeffrey R. Pier, Adrian Pope, Ruth Pordes, Angela Prosapio, Ron Rechenmacher, Thomas R. Quinn,

Gordon T. Richards, Michael W. Richmond, Claudio H. Rivetta, Constance M. Rockosi, Kurt Ruthmansdorfer, Dale Sand ford, David J. Schlegel, Donald P. Schneider, Maki Sekiguchi, Gary Sergey, Kazuhiro Shimasaku, Walter A. Siegmund, Stephen Smee, J. Allyn Smith, S. Snedden, R. Stone, Chris Stoughton, Michael A. Strauss, Christopher Stubbs, Mark SubbaRao, Alexander S. Szalay, Istvan Szapudi, Gyula P. Szokoly, Anirudda R. Thakar, Christy Tremonti, Douglas L. Tucker, Alan Uomoto, Dan Vanden Berk, Michael S. Vogeley, Patrick Waddell, Shu-i. Wang, Masaru Watanabe, David H. Weinberg, Brian Yanny, Naoki Yasuda, and SDSS Collaboration. The Sloan Digital Sky Survey: Technical Summary. AJ, 120(3):1579–1587, September 2000.

[75] Arthur Young, Andrew Skumanich, and Victoria Paylor. Fluorescence-induced Chromospheric H alpha Emission from the K Dwarf Component of V471 Tauri. I. The 1983 Epoch. ApJ, 334:397, November 1988.

[76] T. R. Young, E. Baron, and D. Branch. Supernovae Light Curves : Clues to the Progenitor and Explosions, using Flux-Limited Diffusion. In *American Astronomical Society Meeting Abstracts*, volume 181 of *American Astronomical Society Meeting Abstracts*, page 76.06, December 1992.

[77] M. Zorotovic, M. R. Schreiber, and B. T. Gänsicke. Post common envelope binaries from SDSS. XI. The white dwarf mass distributions of CVs and pre-CVs. A&A, 536:A42, December 2011.